Dynamics of p53 tetramers in live single cells

HARVARD UNIVERSITY
Graduate School of Arts and Sciences

DISSERTATION ACCEPTANCE CERTIFICATE

The undersigned, appointed by the

Committee on Higher Degrees in Systems Biology

have examined a dissertation entitled

Dynamics of p53 tetramers in live single cells

presented by Giorgio Gaglia

candidate for the degree of Doctor of Philosophy and hereby certify that it is worthy of acceptance.

Signature: _____
Typed Name: Dr. Jagesh Shah

Signature: _____
Typed Name: Dr. Timothy Mitchison

Signature: _____
Typed Name: Dr. Philippe Cluzel

Signature: _____
Typed Name: Dr. Sam Lee

Date: February 12, 2014

Dynamics of p53 tetramers in live single cells

A dissertation presented

by

Giorgio Gaglia

to

The Committee on Higher Degrees in Systems Biology

in partial fulfillment
of the requirements
for the degree of

Doctor of Philosophy

in the subject of

Systems Biology

Harvard University
Cambridge, Massachusetts

February 2014

Advisor: Professor Galit Lahav Giorgio Gaglia

DYNAMICS OF P53 TETRAMERS IN LIVE SINGLE CELLS

Abstract

Protein homo-oligomerization is the process through which identical peptides bind together to form higher order complexes. Self-interactions in many cases are constitutive and stable, used as building blocks for biological structures, such as rings, filaments and membranes. Further, homo-oligomerization can also be a regulatory process that influences the proteins' function such as change in transcriptional activities for transcription factors. Innovative methods to measure oligomerization in live cells are needed in order to understand regulation and function of homo-oligomerization in the native cellular context. This thesis examines the case of the tumor suppressor p53, whose homo-tetramerization greatly influences its activity as a transcription factor. We develop methods to quantify p53's self-interaction in individual living cells and follow it in time after DNA damage. The two methods we developed have complementary qualities and different applications. We first use fluorescent correlation spectroscopy to study the molecular events occurring in the first three hours of the p53 in response to double strand breaks. We find that in the absence of stress p53 is present in a mixture of, monomers, dimers and tetramers. When damage is sensed, oligomerization is rapidly induced and nearly all p53 is found bound in tetramers. We combine our data with a mathematical framework to propose the existence of a dedicated mechanism triggering p53 oligomerization independently of protein stabilization. Next, we use bimolecular fluorescent complementation to probe for tetramerization in the longer

timescales of p53's response to ultraviolet radiation. In this context we find that even though the rate of p53 accumulation increases with the dose of radiation, p53 tetramers are formed at a steady rate. We hence propose the existence of an inhibitory mechanism that prevents the oligomerization reaction from following a linear input-output relation. We identify ARC, a known cofactor of p53, as part of this inhibitory mechanism. Downregulation of ARC restore the linear relation between to total and tetrameric p53. Finally, in both experimental setups higher oligomerization lead to an increase in p53 activity, underscoring the connection between regulation of oligomerization and the transcriptional activity of p53 in cancer cells. Collectively, this work emphasizes the importance of precise measurements to investigate the regulation and function of higher order complexes and provides generally applicable methods to quantify homo-oligomerization in live single cells.

Contents

List of Figures

This page intentionally left blank.

Acknowledgments

Thinking back to 6 years ago, when I arrived in Boston to start my phd I remember being excited to start a new chapter of my life but also scared to move to a different country and start a graduate degree in a field completely new to me. Like most phd's my path has been full of up and downs but I was extremely lucky to be surrounded by friends, relatives, co-workers and mentors that made it a fantastic formative experience.

First of all I would like to thank the System Biology Phd Program and the Department of Systems Biology. The dedicated members of the administration, finance, laboratory operation and IT create an extremely well-organized and efficient working environment. I owe a special thanks to Becky Ward for directing such a tight ship yet always being open to answer questions and offer guidance, and to Sam Reed and Shauna Barbosa for organizing the phd program and events and for seamlessly picking up all the balls we students drop, always with a smile. Throughout the years I had the chance to interact with many faculty members inside and outside the department and they have always shown great dedication to science and teaching. I would like to thank the members of my dissertation advisory committee, Peter Sorger, Ralph Weissleder and Jagesh Shah, and of my thesis committee, Tim Mitchison, Philip Cluzel and Sam Lee. I am especially grateful to Jagesh, who has always been supportive and positive even though he had to sit through both my qualifying exams, all my DACs and thesis committee meetings. I feel extremely lucky to have come to work in such an exciting, cooperative and

friendly environment full of outstanding people that taught me so much about science, biology and life.

Big part of why I had such a great experience during my phd is because I was part of the laboratory of Galit Lahav. Galit is special, even unique. On top being a great scientist and communicator, she is an amazing mentor and boss. Her continuous effort to guide each and every one of the members of her lab according to their personality, goals and stage in their career, is inspirational. Galit helped me develop both as a scientist and as a human being; from her I learned to trust myself and my peers, and to balance a productive work schedule with a busy social life. Thank you Galit for mentoring me through all this years, for creating such a pleasant laboratory to work in and for allowing me to be part of it.

The members of the Lahav lab create a wonderful environment. At some point I have been helped and supported by every lab member and I am thankful for all those moments. I will sorely miss the crazy conversations during lunch and the scientific banter that we share every day in lab. Two former postdocs have been especially instrumental in the early stages of my phd. When I first joined the lab Alex Loewer taught me experimental biology from scratch and his dedication inspired me to try my best to teach and support other lab members. I have to thank Eric Batchelor both for his experimental savvy and for introducing me to ballroom dancing, even though he probably couldn't have imagined the huge impact that dancing would have in my life. I had the good fortune of sharing my lab experience with Dr Julia Liu, who has been my ballroom dance partner, my labmate and at one point even lived in the same building as me. Julia has become a little sister for me and my phd would not have been the same without her.

I would like to thank the members of my family for always supporting me along the way. My girlfriend Christina has been at my side for my entire phd; she bore

with my constant sarcasm, the late nights and weekends spent either at work or ballroom dancing. Her playfulness and affection always managed to lift my spirits and put my difficulties in the right perspective. My best friend Guido and my dad Piero always showed huge faith in my abilities, more than I ever had myself. My mother Mariaflavia and my sister Marta have been amazing scientific role models to look up to and one day I hope to match their accomplishments. I have to officially thank my mother for pushing me to learn English when I was a child, even though I resisted in every possible way. Her persistence opened so many doors for me and I am grateful she insisted relentlessly. The love I feel from my family keeps me positive through the hardships, motivated to succeed and makes me feel secure in knowing I always have a home to come back to.

Finally I would like to dedicate this thesis to my maternal grandparents, Fernando and Cettina Di Renzo. Even though they are not here to see me becoming a doctor I know they would be proud.

This page intentionally left blank.

Chapter 1: Background and Introduction

1.1 THE TUMOR SUPPRESSOR P53

The transcription factor p53 is a crucial tumor suppressor in humans and animals. Mutations in the gene expressing p53, TP53, are found in more than 50% of human tumors of various types including cancer of the lungs, colon and leukaemia [1]. Cancer is a set of diseases in which cells abnormally proliferate, survive and invade, leading to tissue malfunction and failure. Whilst the term cancer is used to encompass a broad set of diseases, all of them arise because of accumulation of genomic (and in some instances epigenetic) alterations ranging from single point mutations, chromosome re-arrangements and to genomic loss. The tumor suppressor p53 is a stress-response regulator at the center of a complex protein network that is able to drive a variety of cellular responses such as DNA repair, cell-cycle arrest, apoptosis and senescence. These mechanisms are active in cells to avoid the propagation of genetic mistakes either by allowing time to repair the DNA before

cell division or, if the damage cannot be fixed, by triggering terminal cell fates. Because of the centrality of p53's function in protecting the genetic material, it has been referred to as the "guardian of the genome".

The p53 network consists of a number of proteins involved in sensing cellular stresses, relaying the signal to p53 and enabling p53's activity as a transcription factor. Stresses such as DNA damage, hypoxia and ribosomal stress activate signal mediators that modify and stabilize the p53 protein (Figure **??**). These signaling events activate p53 by altering its half-life, cellular localization, protein conformation and its ability to bind DNA. While there are possible means of regulation of p53 mRNA [2] it does not seem likely that they play a role in p53 dynamics after DNA damage, as the level of p53 mRNA in cells does not change after UV or IR in the timescales of a few days [3, 4]. Activated p53 accumulates in the nucleus where it recruits co-factors, binds to specific DNA sequences called the p53 responsive element (p53 RE) and triggers the transcription activation or repression of target genes. Even though p53 also has important transcription-independent roles [5, 6, 7], the protein works primarily as a tetrameric transcription factor. Over 120 p53-responsive genes have been identified in the human genome though not all of them are regulated in the same conditions [8]. In fact different stresses activate distinct transcriptional programs that include only a subset of these targets.

The core regulation of p53 abundance and activation occurs at the protein level through post-translational modifications. More than 30 residues of p53 are either phosphorylated, ubiquitylated, acetylated, or subject to other types of modifications [1, 9]. The most fundamental mechanism for controlling p53 protein levels occurs through ubiquitylation by Mdm2 (mouse double minute 2) that targets p53 for proteosomal degradation [10]. Even though other two E3 ubiquitin ligases,

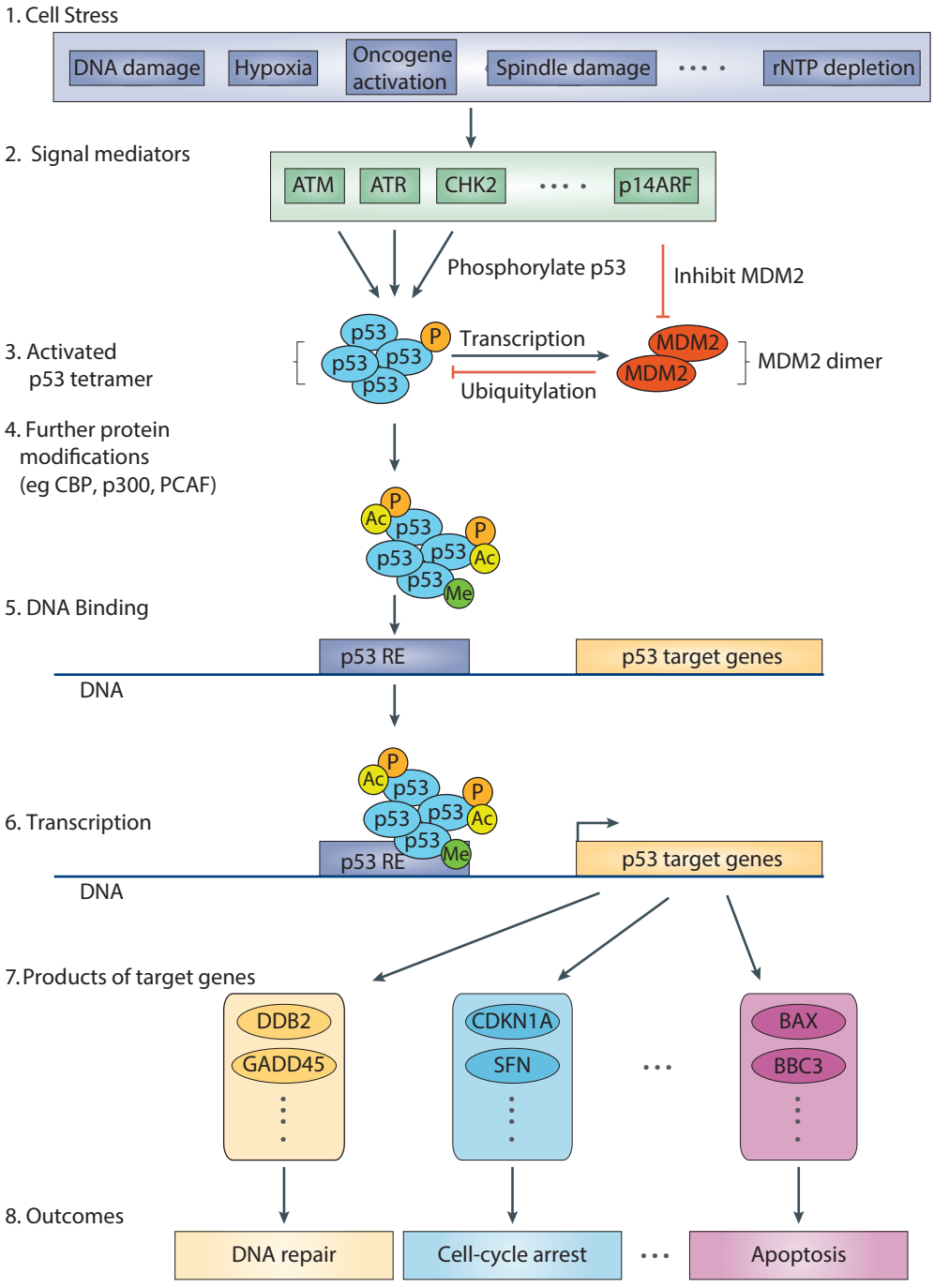
1. Cell Stress
DNA damage
Hypoxia
Oncogene activation
Spindle damage
rNTP depletion
2. Signal mediators
ATM
ATR
CHK2
p14ARF
Phosphorylate p53
Inhibit MDM2
3. Activated p53 tetramer
p53
P
Transcription
Ubiquitylation
MDM2
MDM2 dimer
4. Further protein modifications (eg CBP, p300, PCAF)
Ac
Me
5. DNA Binding
p53 RE
p53 target genes
DNA
6. Transcription
7. Products of target genes
DDB2
GADD45
CDKN1A
SFN
BAX
BBC3
8. Outcomes
DNA repair
Cell-cycle arrest
Apoptosis

Figure 1.1

Figure 1.1: Activation of the p53 pathway after cellular stress. Step 1: Cells are subject to stress. Step 2: Signal mediator proteins trigger p53 activation inducting its phosphorylation and disrupting ubiquitynation by MDM2 (mouse double minute-2). Step 3: p53 is activated by phosphorylation; its half-life increases from minutes to hours leading to p53 protein accumulation. Step 4: p53 is further stabilized by acetyltransferases (CBP, p300, PCAF) and methyltransferases (SET9) which also increase site-specific DNA binding. Step 5: p53 tetramers bind to p53 response elements (RE) in the DNA. Step 6: p53 regulates the expression of target genes, both mediating transactivation and repression of target genes. Step 7: The products of the genes regulated by p53 are involved in various pathways. Step 8: Transcriptional programs fundamental for tumor suppression are triggered by p53 include DNA repair, cell-cycle arrest, senescence and apoptosis. ATM, ataxia telangiectasia mutated; BAX, BCL2-associated X protein; BBC3, BCL2-binding component-3; CDKN1A, cyclin-dependent kinase inhibitor-1A; CHK2, checkpoint kinase-2; DDB2, damage-specific DNA-binding protein-2; GADD45α, growth arrest and DNA-damage inducible α; p14ARF; SFN, stratifin; (Figure adapted from [8])..

Pirh2 and Cop1, seem to have redundant function to Mdm2, the latter is the main regulator of p53, as shown by compelling biochemical evidence [11] and by the observation that $Mdm2^{-/-}$ mice are not viable but can be rescued by double p53 knockout [12]. Prior to degradation, mono-ubiquitylation by Mdm2 is also responsible for nuclear export of p53 [13]. Phosphorylation is the most frequent modification; after stress a vast array of kinases phosphorylates p53 at as many as 17 residues. In general both phosphorylation and acetylation are thought to stabilize the p53 protein and increase its affinity to specific promoters. However, even though the global impact of post-translational modifications in p53 function is clear, specific modifications were suggested to play a different role in p53 function and the effect of individual modifications is unclear for most of them. Additionally most modifications are reversible and they can transiently be added and removed after stress or during specific cell-cycle phases [14]. Each modification is hence kept in a finely tuned on-off balance resulting in a "complex barcode" of modifications state that

shifts dynamically and enables p53 to continuously integrate signals [1].

The dynamic control of p53 activity is also achieved by a series of transcriptional feedbacks [15]. While most of the transcriptional targets of p53 accomplish key cellular functions and stress responses, some are involved in p53 regulation. The negative regulators of p53, the ubiquitin ligases Mdm2, Pirh2 and Cop1 are all transcriptional targets of p53 and their expression in enhanced upon stress [16, 17, 18]. Important p53-responsive gene such as PTEN, p19/p14 ARF and cyclinG regulate p53 by feedbacks acting on Mdm2. Finally other targets modify the activity of signal mediators upstream of p53, for example,the phosphatase Wip1 that targets ATM (see DNA damage section below).

As mentioned above, p53 works primarily as a tetrameric transcription factor. In this work I focused on the formation of p53 homo-tetramers in response to two DNA damaging agents, ultraviolet and ionizing radiation. In the next sections I will introduce the p53 response to DNA damage and what is known about p53 homo-tetramerization.

1.2 THE P53 RESPONSE TO DNA DAMAGE

DNA damage is an alteration to the chemical structure of the DNA, either of the backbone or of the bases. Chemical modifications include the break in the DNA strands, intra- and inter-strand crosslinking and loss of base-pairing information, all of which lead to stalled replication forks or incorrect DNA replication. Damage to the DNA occurs naturally in cells and it is continuously fixed by one of the DNA repair mechanisms. However, if not properly dealt with, errors in the fidelity of DNA replication deteriorate the genetic information. The propagation and accumulation of loss of information eventually leads to cell malfunction and cancer. Hence timely detection of DNA damage and its efficient repair represents

a fundamental cellular activity.

Sources of DNA damage are both endogenous and exogenous to cells. Normal cellular metabolism releases reactive oxygen species, reacting nitrogen species and alkylating agents that chemically modify DNA. Damaging chemical agents are also absorbed from the environment, usually referred to as carcinogens. External sources of damage also include ultraviolet radiation and ionizing radiation that both cause the release of reactive oxygen species on top of having direct DNA damaging effects.

Ultraviolet radiation (UV) induces the formation of pyrimidine dimers [19]; these are detected and excised by the nucleotide excision repair mechanism (NER). If this procedure fails, replication is taken over by the translesion DNA synthesis machinery that replicates the DNA bypassing the lesion, a failsafe and error-prone mechanism. In absence of efficient repair UV lesions are devastating. Germline mutations in the component of the NER are associated with xeroderma pigmentosum (XP), an autosomal recessive genetic disorder that leads to hypersensitivity to UV [20]. Homozygous XP individuals develop carcinomas at a young age and rarely live past 20 years of age [21]. In response to UV radiation, p53 is activated and was shown to predominantly trigger apoptosis [22, 23, 24].

Ionizing radiation (IR) directly ionizes and breaks DNA strands. When two single-stranded breaks occur with 10 base pairs of each other they form double-strand breaks (DSB), the most dangerous form of DNA break. Similar double strand breaks can be induced chemically using radiomimetic drugs. In this study I used neocarzinostatin (NCS), a drug permeable to cells in culture that cleaves the DNA backbone with free radical attack causing damage closely mimicking ionizing radiations [25, 26]. In response to IR and radiomimetic drugs, p53 triggers a transcriptional program that causes cells to arrest the cell cycle and to undergo

senescence.

Ultraviolet and ionizing radiation activate the p53 network through different pathways (Figure 1.2). Single-stranded DNA exposed by stalled replication forks after UV activates the ataxia telangiectasia and Rad3-related protein (ATR) and its co-factor and activator ATRIP. ATR phosphorylates p53 directly on Ser15 and Ser37 [27], and activates two other kinases, checkpoint kinase 1 (Chk1) and p38, that in turn phosphorylate p53 on serine residues 15, 20, 33, 46 and 392 [9, 24, 28]. Instead DSBs lead to the activation of the kinases ataxia telangiectasia mutated (ATM) and checkpoint kinase 2 (Chk2) [29, 30], which phosphorylate p53 at multiple residues including serine 6, 9, 15, 20 and 366 [9, 31].

In the absence of stress, many tissues have low levels of p53 protein. Mdm2 continuously ubiquitylates p53 and targets it for degradation, resulting in a half-life of 6-20 minutes [8]. Post-damage phosphorylations on p53 disrupt the binding to Mdm2 and p53 protein accumulates. Since Mdm2 is itself a target of p53 transcriptional activity, the level of Mdm2 eventually increases until it is enough to overcome the stabilization of p53; this negative feedback leads to downregulation of p53 and to pulsatile dynamics [32]. In the past ten years the Lahav laboratory and other groups have characterized the pulsatile dynamics of p53 protein in culture cells after DNA damage using fluorescence microscopy of GFP-tagged p53. This is possible since the dynamics of p53 protein are mostly modulated at the protein level.

1.3 Dynamics of p53 in single living cells

The dynamics of p53 were shown to depend on the specific DNA damage. After UV radiation p53 undergoes a single pulse of accumulation whose magnitude and duration is dependent on the radiation dose [33]. While at population level

the dynamics of p53 protein after IR appear to display multiple damped pulses [34], single cells studies show that p53 undergoes a series of pulses with conserved height and width [35, 36]. However the cells slowly lose synchrony of pulsing and stop pulsing at different times, effects that are masked at cell-population level.

Recent work for the Lahav laboratory has shown that the difference in p53 dynamics after UV versus IR is due to a second negative feedback driven by another p53 transcriptional target, Wip1 [35]. Wip1 is a phosphatase that dephosphorylates p53, decreasing its stability. In response to IR, Wip1 is also able to target ATM, inhibiting its activity and disrupting the signaling upstream of p53. Since ATR's activity does not depend on phosphorylation, ATR is unaffected by Wip1 and this negative feedback does not occur after UV (Figure 1.2 adapted from [33]).

The total level of p53 in cells is an important indicator of its activity but it does not capture its functional state [37]. Post-translational modifications are a prime example of how the state of p53 majorly changes its activity level and the subsequent cellular outcome. Another aspect of p53 that changes its activity is its homo-oligomerization state. In fact, p53 forms homo-tetramers *in vitro* and *in vivo* and these represent the functional unit of p53 activity. In the next sections I outline what is known about p53 tetramerization, the open questions in the field and the challenges to study it in live cells.

1.4 HOMO-OLIGOMERIZATION OF P53

Protein homo-oligomerization is the formation of specific protein aggregates of multiple identical subunits. Homo-oligomerization is extremely common in nature: recent studies have shown that around 60% of proteins in the Protein Data Bank and more than 2/3 of human enzymes forms homo-oligomers [38, 39]. Oligomerization can serve structural purposes, for example in viral capsids where the self-

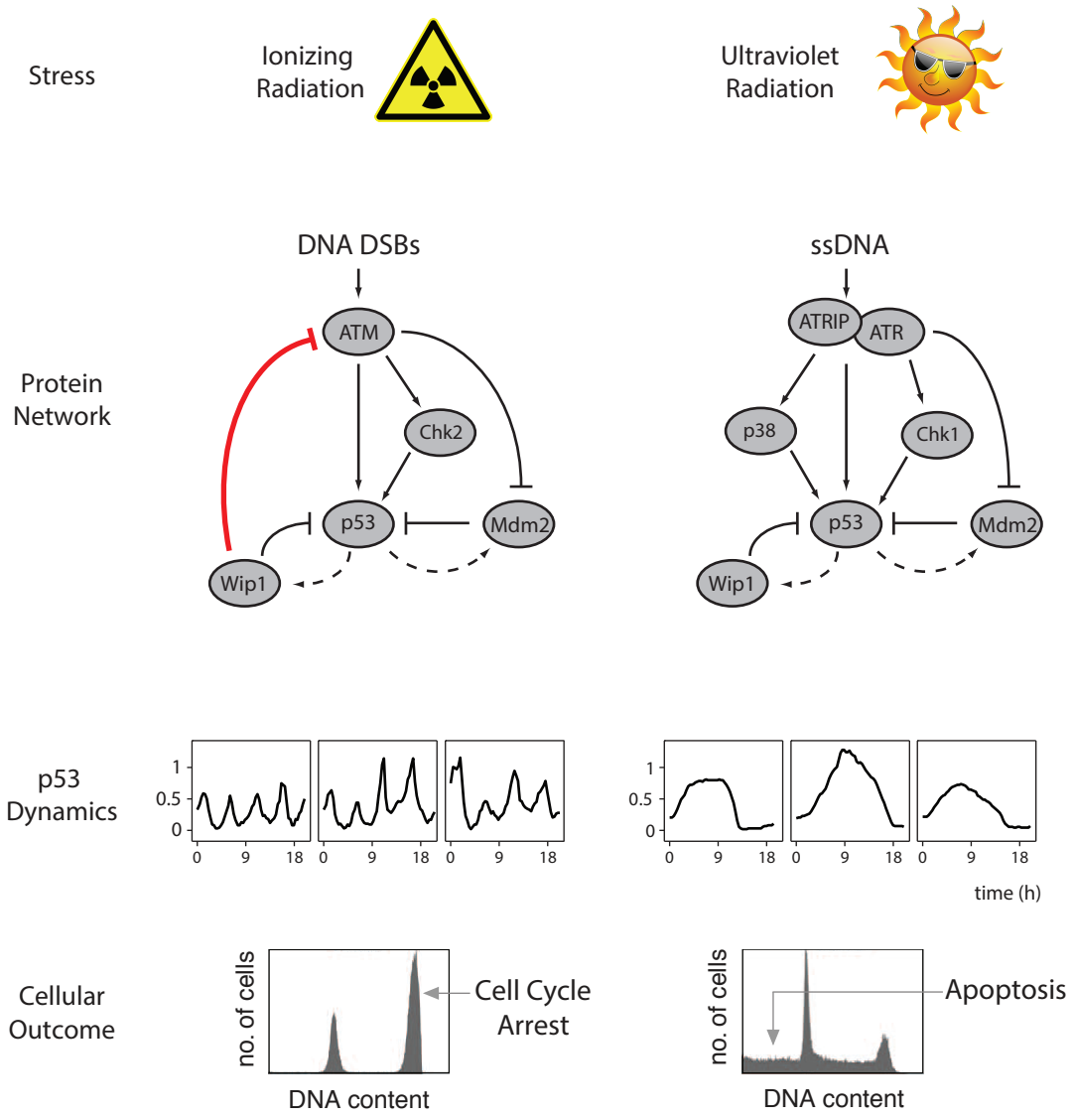

Figure 1.2: Effects of DNA damage through the p53 pathway. Different sources of DNA damage, such as ionizing radiation (IR) and ultraviolet radiation (UV), activate the p53 pathway through distinct signals, double strand breaks and exposure of single stranded DNA respectively. These signals engage overlapping yet separate networks of proteins regulating p53, leading to different dynamics of p53 protein levels after stress. These dynamics trigger distinct cellular fates (adapted from [22, 33]).

assembly of a single (or a few) proteins allows formation of a 3-dimensional structure. These complexes are extremely stable with oligomeric dissociation constant in the nanomolar range [40]. In many other instances oligomerization is a regulated step that changes the function of the protein, as for the case of G-protein coupled receptors [41], C/EBP family transcription factors [42] and the apoptotic protein Bax [43].

The p53 protein forms homo-oligomers through a C-terminal small protein domain called the tetramerization domain (TD) spanning amino acids 326-355 (Figure 1.3A). The structure of the TD consists of a beta-sheet and an alpha-helix separate by a sharp turn (Figure 1.3B). The domain forms homo-dimers by anti-parallel interactions between the beta-sheets and by anti-parallel helix packing (red and yellow chains in Figure 1.3B). Once primary dimers are assembled the tetramerization interface forms by the alpha-helices, four of which come together in a 4-helix tetrameric bundle [44, 45]. Since dimerization is required before tetramerization, tetramers are considered "dimers of dimers" and p53 does not exist in trimeric form. While other parts of the protein are known to create homo-oligomeric contact points, the tetramerization domain is central to the formation of oligomers as in its absence oligomers are not observed [46, 47].

Purification of full-length wild-type p53 has proven extremely challenging and a complete protein structure of wild-type is not available. *In vitro* and structural studies either use fragments of the p53 protein to isolate specific domains [45, 48] or use super stable mutants developed in the Fersht laboratory in Cambridge UK [49, 50, 51, 52]. Tetramerization of p53 has been studied with many *in vitro* methods that yielded to a comprehensive understanding of the reaction.

Dimers of p53 form at extremely low concentrations; their dissociation constant has only recently been measured to be Kd = 0.55 ± 20 nM [53]. Protein folding stud-

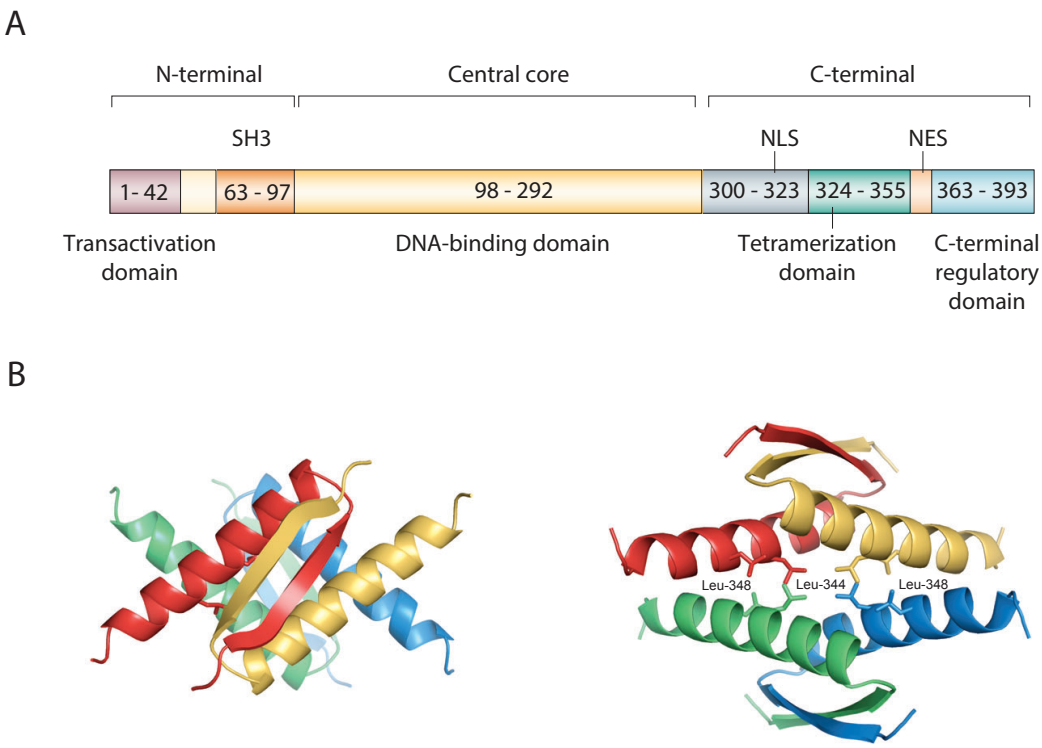

Figure 1.3: Scheme of the p53 protein domains and structure of the tetramerization domain. **A.** The p53 protein spans 393 amino acids usually divided into three functional domains. The N-terminal domain is made up of the transactivation domain and a Src homology 3-like (SH3) domain. The central core consists only of the DNA-binding domain through which it contacts the DNA directly. The tetramerization domain resides in the C-terminal end together with a nuclear localization and export signals (respectively NLS and NES) and a regulatory domain (panel adapted from [9]) **B.** Ribbon model of the structure of tetramerization domain of p53. Two different orientations are shown and each subunit of the domain is colored differently. On the right side panel the side chains of key residues used for disrupting the tetramerization reaction (L344 and L348) are highlighted. Panel adapted from [44].

ies have shown that the dimerization reaction occurs while the peptide folds, with the protein passing from an unfolded monomeric state straight to a folded dimeric state [54]. Interestingly, an *in vitro* translation study by Nicholls et al. showed that when two mRNA constructs producing distinct p53 proteins are translated at the same time, only homo-dimers are detected [55]. This hence implies that dimerization occurs co-translationally, in proximity of the polysome, while the protein is being translated. Once dimerization occurs the two alpha-helices of the TD form an hydrophic patch responsible for tetramerization [44]. Tetramerization is markedly less stable than dimerization with a K_d ~ 200nM – 2μM [53, 56, 57, 58]. Based on measurement of p53 protein concentration of 140nM (measured in MCF7 cell by ELISA [59]) it was suggested that, in absence of stress p53, is mainly dimeric in cells.

1.5 Regulation of tetramerization

p53 binds DNA as a tetramer [60]. DNA sequences containing the p53 responsive element offer a surface for cooperativity facilitating tetramerization [56]. Certain post-translational modifications have been shown to enhance tetramerization, namely Ser392 phosphorylation [58] and Tyr327 nitration [61], while others, like acetylation of C-terminal lysines, inhibit oligomerization [62]. Modifications of p53 can also affect indirectly the level of tetramerization by recruiting co-factors of p53: for example phosphorylation of Ser366 or Thr387 was shown to recruit members of the 14-3-3 protein family that increase p53 tetramerization [57, 63].

Co-factor binding also plays a crucial role in the regulation of p53 oligomerization. The binding of certain co-factors induces tetramerization, like the aforementioned 14-3-3σ, the redox factor-1, Ref-1 [64] and p300 [65]. Other proteins instead interact directly with the tetramerization domain of p53 and inhibit competitively

tetramerization or even dimerization. This category includes the members of the S100 family [66] and the apoptotic repressor with CARD domain (ARC) [67].

1.6 Function of p53 tetramerization

The most important feature of p53 tetramerization is that it is essential for efficient DNA binding and hence for its transcriptional activity. Kawaguchi and coworkers extensively tested the transcriptional capacity of a library of mutants in the tetramerization domain with a reporter system in yeast [68]. Their study showed that mutations that rendered p53 monomeric lead to a complete loss of transcriptional activity while some mutants that formed dimers but not tetramers retained a low capacity of activating target genes. Furthermore, *in vitro* testing showed that dimers of p53 can still bind DNA but with two orders of magnitude lower binding affinity [60].

Two germline mutations in the tetramerization domain that cause complete loss of oligomerization, R337C and L344P, have been strongly linked to Li-Fraumeni syndrome, a disease characterized by early onset of cancer [69]. Elevated incidence of another germline p53 tetramerization mutation, R337H, has been observed in children affected by adrenocortical carcinoma (ACC) in southern Brasil [70]. While cancer mutations commonly target DNA binding domain of p53, somatic mutations in the TD have not been frequently observed in cancers. A higher incidence of mutations in the TD would be expected, since in cells the loss-of-function phenotype of TD mutants is similar to that of mutants in the DNA binding domain. However a plausible hypothesis is that the loss of oligomerization ability caused by mutation in one allele of p53 is unable to affect the function of the wild-type p53, while DNA binding mutants that retain the capacity to oligomerize can exert a dominant-negative effect [71, 72].

For this study, amongst the mutations that affect tetramerization I selected two point mutations in residue Leu344 as a control (Figure 1.3B). Alanine substitution at this residue (L344A) renders the p53 protein unable to form tetramers while retaining the capacity of efficiently form dimers [54, 73]. Since leucine 344 is part of the alpha helix in the TD, mutation to proline disrupts the structure of the helix and of the entire TD, making p53 L344P strictly monomeric [74].

Besides DNA binding, p53 tetramerization is also important for post-translational modifications and cellular localization. Specifically phosphorylation of several serines (residues 6, 9, 46 and 315) and acetylation of C-terminal lysine 382 is abrogated in oligomerization defective mutants [75, 76]. Moreover, tetramerization is thought to mask the nuclear export sequence (NES, Figure 1.3A) preventing access to the export machinery and causing p53 to accumulate in the nucleus [77].

While the tetramerization reaction has been extensively and successfully studied *in vitro* in the test tube, our understanding of the regulation and function of p53 oligomers in live cells is extremely limited. First of all we still do not know the stoichiometry of p53 in cells. Given that tetramerization is altered by multiple post-translational modifications and co-factors, some of which facilitate oligomerization while other disrupt it, the *in vitro* measurements of dissociation constants can only be indicative. Further, the role of tetramerization has been explored by either mutating p53 or by silencing and overexpressing possible regulators. However it is still unclear what happens to the oligomerization state of p53 after a stimulus, such as DNA damage. This question is further complicated by the fact that the total p53 protein itself undergoes complex dynamics after DNA damage that would affect the stoichiometric balance even in absence of specific regulation of the oligomerization reaction.

1.7 MEASURING TETRAMERIZATION TO QUANTIFY THE ACTIVE FORM OF P53

One reason for why the above questions have remained unanswered is that measuring protein self-interactions in cells is challenging. The common methods to identify protein interaction rely on the putative binding partners differing in size or charge. On top of this, most techniques are able to detect homo-dimers but not any higher-order oligomer. The aim of my work was to quantify p53 tetramerization accurately in live cells. Hence this required the development of experimental techniques that are discussed in the following paragraphs.

In general, protein quantification in live cells relies on fluorescent protein tagging. Tagged p53 has previously been shown to accurately report for endogenous p53 and it has been used to study its dynamics in single cells [32, 35, 36]. In order to extend fluorescent reporters to probe for protein oligomerization a technique that allows resolution of the protein aggregates composition is required. To this extent I used fluorescence correlation spectroscopy (FCS) to measure the aggregation state of CFP-tagged p53 in single live cells. Another possible method to measure oligomerization is to use two p53 constructs differentially tagged and probe for their interaction, for example using complementary fragments of fluorescent proteins that only become fluorescent upon binding. This is called bimolecular fluorescence complementation (BiFC) and it is the second method I used to measure p53 oligomerization.

1.7.1 Fluorescence Correlation Spectroscopy (FCS)

FCS is one of the techniques used to analyze the fluctuations in fluorescent intensity of a small sample volume; there are other ways of analyzing such data like photon

counting histogram and molecular brightness analysis, and collectively this group of methods is called fluorescent fluctuation spectroscopy (FFS) [78, 79, 80]. These methods rely on probing a solution of fluorophores and measuring the fluorescence intensity of a small subvolume in time with micro- to millisecond resolution. The variations of the intensity measurement, referred to as fluctuations, come from the movement of fluorescent molecules to and from the volume. As the diffusion of single fluorophores produces fluctuations of smaller amplitude than multiple fluorophores bound together, the aggregation state of these molecules can be calculated from the analysis of the fluctuations.

In order to maximize the chances of successful a FCS experiment, the measurement requires the greatest accuracy possible and hence a specific experimental setup is needed (Figure 1.4). Firstly a small observation volume of ~ 1 fL is required. This can be obtained by confocal microscopy or two-photon excitation, but the latter is usually preferred as it lowers photobleaching. Instead of to a CCD camera the light collected from the sample is then directed through a photodetector, like a photomultiplier tube (PMT) or avalanche photodiode (APD). These devices have high gain and low dark counts, in order to avoid missing any photon hitting the sensors, and fast response time to be able to respond to high frequency of photon excitation [81]. Finally the data is stored in a photon counting acquisition card that keeps the complete history of photon counts events on which the analysis is performed.

Different types of analysis can be performed on the photon counts data, depending on the information to be extracted. FCS consists in binning the data in time and calculating the autocorrelation of the resulting time trace. The details of the setup and analysis I use can be found in the Materials and Methods section of Chapter 2 of this study. FCS and related fluctuation techniques have been used in cells and

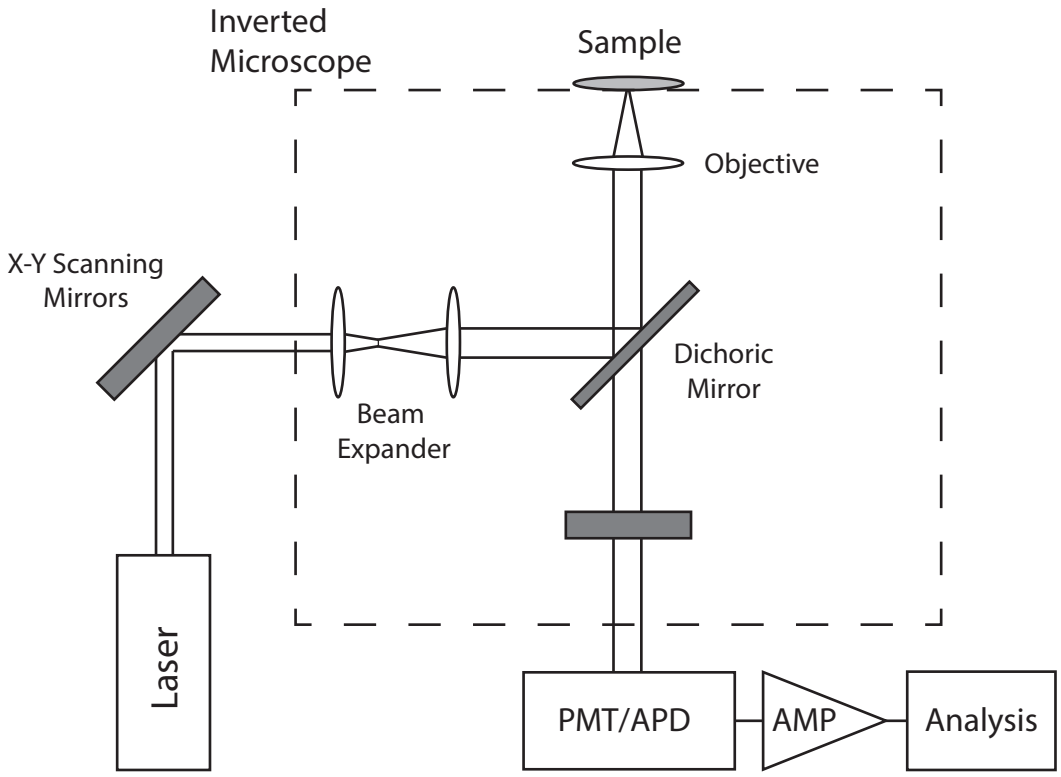

Figure 1.4: Schematic of two-photon FFS instrument. A laser provides two-photon excitation light source. The excitation light is sent to the inverted microscope. Either a PMT or APD detects the fluorescence generated by the two-photon excitation. The data is the subect of analysis by fluorescent correlation spectroscopy or similar techniques (adapted from [81]).

model systems to study protein aggregation [82], complexes of viral proteins like Gag and Vpr [83, 84], formation of membrane lipid layers [85] and receptor homomeric aggregates [86]. These studies, however, use the diffusion coefficient to draw conclusions regarding interaction and oligomerization. In this work I used FCS to calculate the so-called "particle brightness", a parameter that reports for the stoichiometry of fluorophore aggregates travelling through the volume: this analysis was pioneered by the group of Enrico Gratton (Department of Physics, University of Illinois, Urbana Champaign) who also showed that the method is appropriate to measure oligomerization in human cells [79, 87]. In Chapter 2, I employed the particle brightness to study the activation of p53 tetramerization after DNA double strand breaks.

While FCS is a powerful and precise technique, its application to live specimens has some limitations. The experimental setup is not optimal for human cells allowing only 3-5 hours long measurements before stress-response pathways become active. Since the dynamics of p53 after DNA damage are in the timescale of hours [36], only the initial events of p53 activation can be observed by FCS. Moreover, the length of the measurements (~5 minutes per cell per timepoint) does not allow collecting more than 5-8 cells per experiment. For these reasons I developed a second method to quantify p53 oligomerization in single cells that makes use of epifluorescent microscopy.

1.7.2 Bimolecular Fluorescence Complementation (BiFC)

Protein-fragment complementation is a technique for which a reporter protein is split in two fragments that can bind to each other and reconstitute the original protein. The fragments of the protein are not active alone but when the full protein is reconstituted its activity is restored. Common examples of proteins used for this

purpose are enzymes like dihydrofolate reductase and beta-lactamase [88, 89] and the split version of the transcription factor Gal4, the base of the yeast two-hybrid system to test protein-protein interactions.

The fluorescent version of protein complementation is called bimolecular fluorescent complementation (BiFC) and it involves splitting a fluorescent protein and disrupting the fluorescent beta-barrel core [90]. The resulting two fragments are not fluorescent in isolation and have low affinity for each other. Hence they do not bind each other unless they are tagged to interacting proteins. When the latter binds the non-fluorescent fragments are kept in close proximity allowing for the protein to reconstitute and for the fluorescent core to mature [91].

In order to use BiFC to measure oligomerization dynamics, specific controls are required. First, even though the fluorescent fragments affinity is low, there still could be unspecific binding and hence background fluorescence. Moreover, compared to similar methods like FRET, a major drawback of BiFC is that the reconstitution reaction is irreversible as the fragments are not able to separate again. Hence it is important to test whether the tagging of split fragments to the protein of interest does not modify its dynamics. Lastly BiFC theoretically reports only for dimerization of the protein of interest not for higher order oligomers, like tetramers.

In the case of p53 I overcame these challenges as follows: the oligomerization mutants described above (p53 L344A and p53 L344P) served as controls to calculate the background fluorescence coming not only from unspecific binding but also from sources other than the tetramerization domain of p53. Secondly, the dynamics of p53 after DNA damage are extremely well characterized and hence it is possible to test directly the effect of the split fluorescent tagging on the p53 behavior after stimulus [33]. Finally, p53 dimers were shown form co-translationally *in vitro* [55]. This implies that both monomers in each dimer of p53 are translated from

the same mRNA and carry the same fragment of the fluorescent protein. Since the fragments are not symmetric [90] the dimers would not be able to form a fluorescent protein until two dimers carrying complementary fragments come together as a tetramer. In this scenario the BiFC setup reports directly for tetramers. In Chapter 3, I employed a BiFC setup to test the co-translationality of p53 dimers in cells and to measure the dynamics of total p53 protein and p53 tetramers in live single cells after UV radiation.

Chapter 2 : Activation and Control of p53 tetramerization

Homo-oligomerization is found in many biological systems and has been extensively studied in-vitro. However, our ability to quantify and understand oligomerization processes in cells is still limited. We used fluorescence correlation spectroscopy (FCS) and mathematical modeling to measure the dynamics of the tetramers formed by the tumor suppressor protein p53 in single living cells. Previous in vitro studies suggested that in basal conditions all p53 molecules are bound in dimers. We found that in resting cells p53 is present in a mix of oligomeric states with a large cell-to-cell variation. After DNA damage, p53 molecules in all cells rapidly assemble into tetramers before p53 protein levels increase. We developed a model to understand the connection between p53 accumulation and tetramerization. We found that the rapid increase in p53 tetramers requires a combination of active tetramerization and protein stabilization, however tetramerization alone is sufficient to activate p53 transcriptional targets. This suggests triggering tetramerization as a new mechanism for activating the p53 pathway in cancer cells. Many other transcription factors homo-oligomerize, and our approach provides a new way for probing the dynamics and functional consequences of oligomerization.

2.1 INTRODUCTION

Homo-oligomerization, the formation of a protein complex out of identical components, is extremely common in nature; in E. Coli it is estimated that 35% of proteins form homo-oligomers [40] with an average of 4 subunits per complex. In yeast and human cells many transcription factors undergo homo-oligomerization, which has been shown to be crucial for their function [92]. The molecular dynamics of oligomerization have been studied for some proteins *in vitro*, but no study has quantified discrete numbers of oligomers in a dynamic oligomerization process in live single cells. Here we focus on the homo-tetramers formed by the tumor suppressor p53 and quantify the fraction, dynamics and function of homo-oligomers in single living cells in response to DNA damage.

p53 is a stress-response transcription factor that orchestrates cell fates decisions such as cell-cycle arrest, senescence and apoptosis. Tetramerization of p53 is required for its direct binding to DNA [48, 93]. Mutations in the p53 tetramerization domain (326-356 aa) lead to a reduction in, or loss of, its transcriptional activity in cells [68] and were shown to cause early cancer onset, known as Li-Fraumeni syndrome [70, 74].

In *in vitro* studies, p53 first assembles into homo-dimers with a K_d of ~1 nM [53]. These dimers then come together in tetramers with a K_d of ~100nM-1µM [53, 56, 57, 58]. The K_d of tetramerization *in vitro* can be lowered by specific post-translational modifications [57, 58, 94]. Based on these measurements and the estimated p53 concentration in cells of 140 nM [59] it has been proposed that p53 should be primarily dimeric in basal conditions and that it forms tetramers in stressed conditions [9]. However there is currently no direct experimental evidence for this in cells.

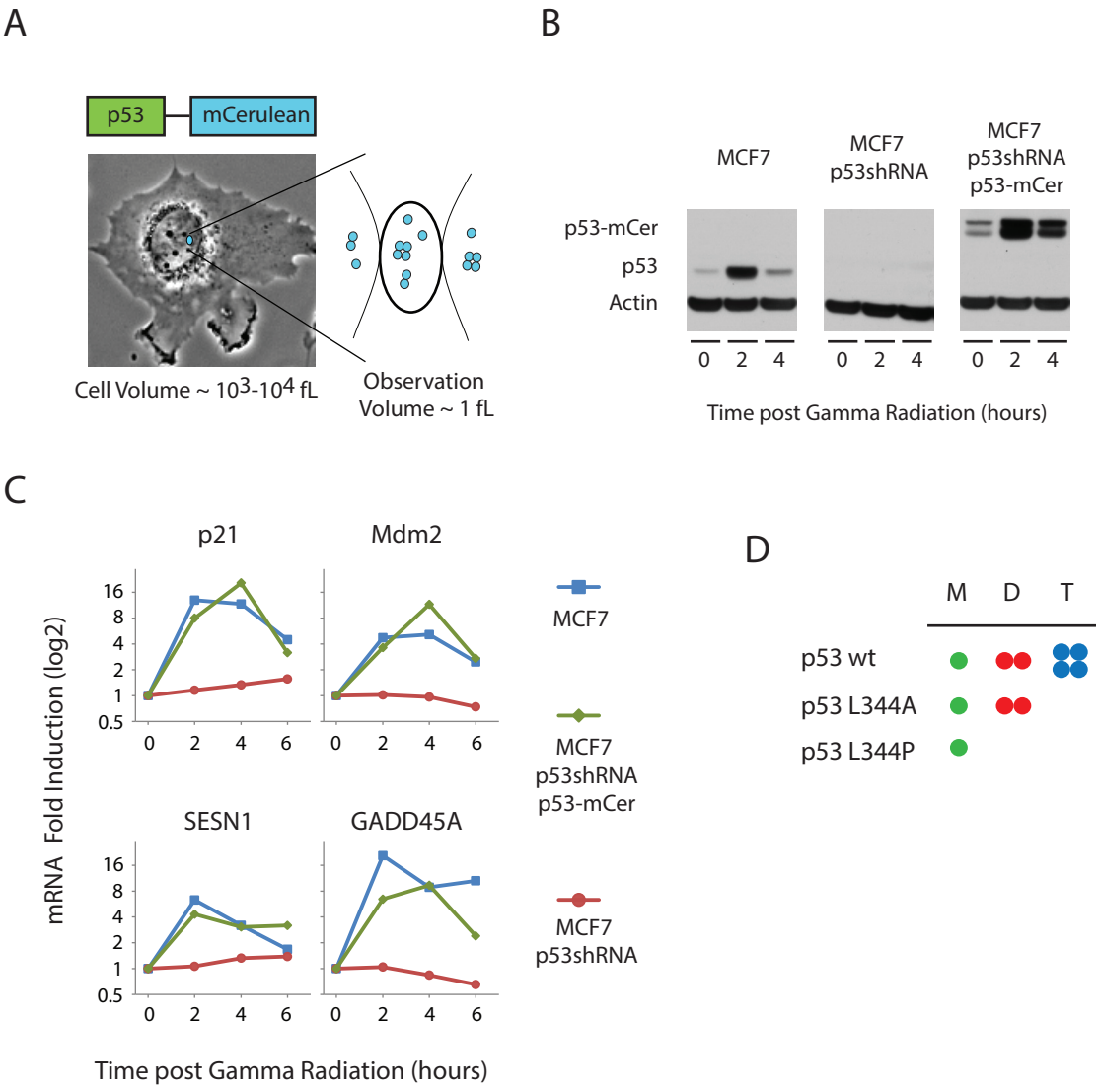

Figure 2.1: Experimental setup and controls for p53 functionality A. Schematic view of FCS measurement. The FCS measurements were obtained with a two-photon excitation laser in the nucleus of live cells. The laser creates an observation volume of ~ 1 fL, through which fluorescently labeled p53 molecules diffuse. C-terminal tagging of p53 with mCerulean does not disrupt the dynamics and function of p53. **B.** p53 levels were measured using immunoblots in parental MCF7 cells, MCF7 cells silenced for p53 (p53 shRNA) and cells expressing p53 tagged to mCerulean. **C.** mRNA levels of p53 target genes measured using qPCR. The reintroduced tagged p53-mCerulean is able to induce expression of p53 target genes. **D.** Wild-type p53 forms dimers ("D") and tetramers ("T"). Mutant p53 L344A forms dimers but no tetramers and p53 L344P mutant is only monomeric ("M").

We used fluorescence correlation spectroscopy (FCS) to quantify the fraction of p53 monomers, dimers and tetramers in living single cells in a basal state and post DNA damage. FCS is widely used *in vitro* to measure protein homo-oligomerization, including p53 tetramerization [53, 93] but has only rarely been used in living cells for this purpose [95]. FCS provides direct measurements of the intensity and brightness of fluorescent molecules [96]; the intensity reports the numbers of fluorescent molecules in the volume and therefore provides a measure of total protein concentration. The brightness captures the average fluorescent intensity of p53 aggregates, hence higher brightness indicates higher oligomerization state (Figure 2.1A). Note that the brightness captures only the interactions between fluorescently labeled molecules and hence it is not affected by non homo-oligomeric binding interactions, even when these might affect the diffusion rate (see Methods).

2.2 RESULTS

2.2.1 p53 is present in a mixture of oligomeric states in cells.

For FCS to provide an accurate measure of p53 oligomerization state, all p53 molecules must be fluorescently labeled. We therefore established a cell line silenced for endogenous p53 [97] to which we reintroduced an exogenous p53 tagged with mCerulean, a monomeric version of CFP (Figure 2.1B). Fluorescently tagged p53 was previously shown to mimic the dynamics of endogenous p53 in response to DNA damage [35] and here we show that its function as a transcription factor is analogous to wild-type p53 (Figure 2.1C). We also constructed cell lines expressing two p53 mutants, which have been extensively tested *in vitro*: p53 L344A - a mutant that cannot form tetramers but does form dimers and p53 L344P - a mutant that cannot form dimers or tetramers and is therefore only monomeric (Figure 2.1D).

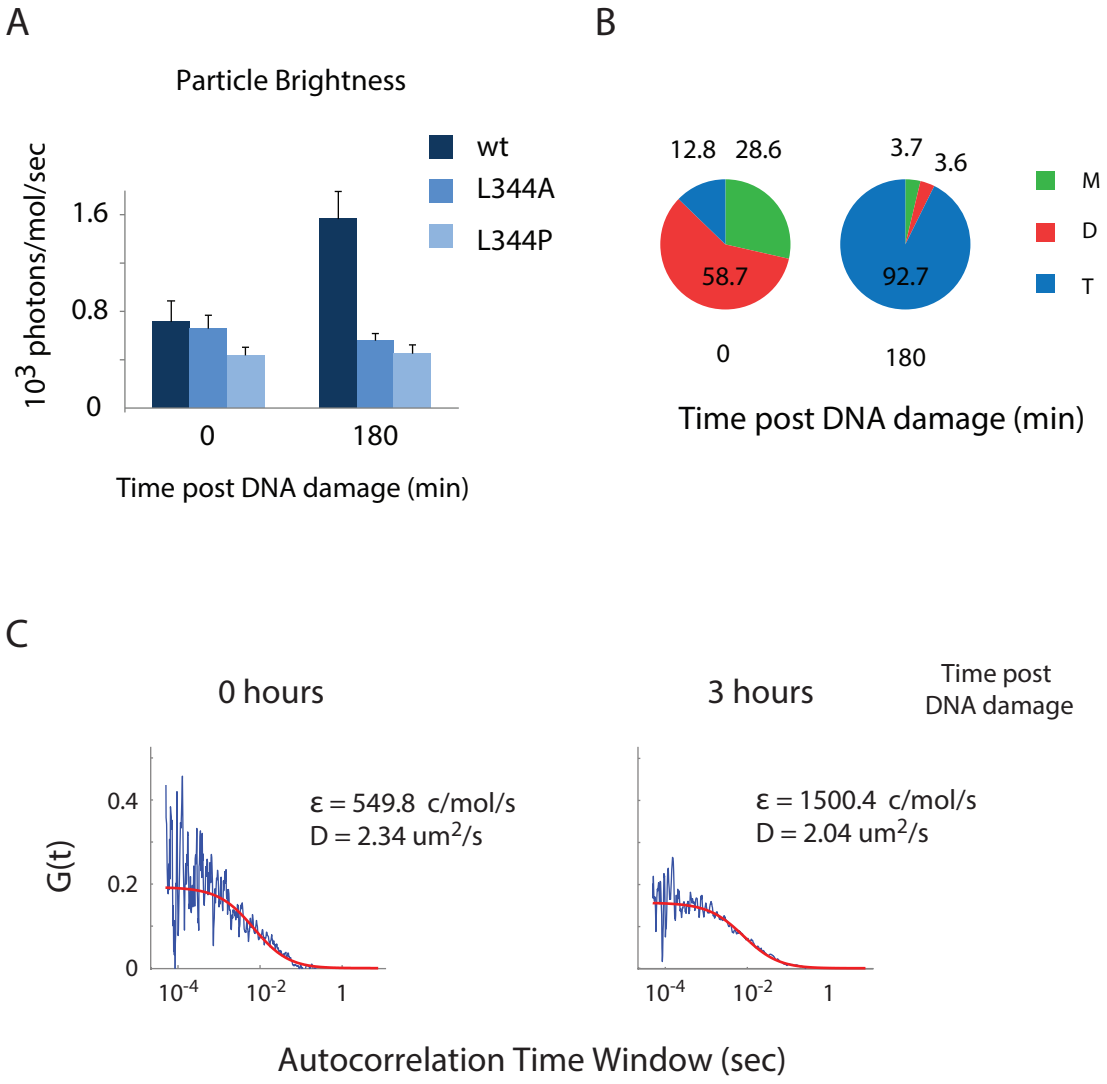

Figure 2.2: Distribution of p53 oligomeric states before and after DNA damage A. p53 oligomerization is induced after DNA damage. The oligomerization state is represented by the particle brightness. **B.** Percentages of p53 monomers, dimers, and tetramers in basal conditions (left) and after DNA damage (right). **C.** An example for FCS autocorrelation traces and fits in one cell. Autocorrelation G(t) is calculated by averaging five 30 second measurements at a specific time point after DNA damage. The autocorrelations were fit to theoretical curves assuming Brownian diffusion (red line). The values for the diffusion constant 'D' and brightness 'ε' for the correspondent traces are calculated by the fitting of the autocorrelation curves.

We measured the particle brightness of wild-type p53 and the two mutants at rest and after DNA damage induced by the radiomimetic drug NCS (Figure 2.2). The increase in brightness following DNA damage results from tetramerization since only the brightness of wild-type p53 increased (Figure 2.2A). We used the brightness of the monomeric mutant L344P, $\varepsilon_{(mono)}$, to calculate the relative abundance of p53 in each oligomeric state by breaking up the intensity I and the number of molecules N into the specific numbers of p53 monomers M, dimers D and tetramers T using the following equation:

$$\textit{Particle Brightness} = \varepsilon = \frac{<I>}{<N>} = \varepsilon_{(mono)} * \frac{1+2*\frac{D}{M}+4*\frac{T}{M}}{1+\frac{D}{M}+\frac{T}{M}}$$

The FCS brightness analysis was confirmed using photon counting histogram analysis (PCH) [78] on the fluorescence fluctuation data (Figure 2.3A). We confirmed the reliability of the FCS brightness analysis for quantifying oligomerization by showing that the brightness of fluorescent tandem dimers is double the brightness obtained from monomers in cell lysates using both FCS and PCH analysis (Figure 2.3B and C). Notably control cells lacking fluorescent reporter showed minimal background and no FCS signal (Figure 2.3D and E) and photobleaching was found to be minimal (<10%) in our experimental setup (Figure 2.3F).

Based on the particle brightness obtained from the p53 mutants and the wild-type p53 (Figure 2.2A) we calculated that at rest the majority of p53 is bound in dimers with 29% unbound monomers and 13% tetramers (Figure 2.2B). Note that the measured mean concentration of p53 in basal conditions (397nM) was much higher than the dimeric dissociation constant of ~ 1 nM measured *in vitro*. Yet nearly 30% of p53 molecules are still monomeric, suggesting that additional factors control p53 dimer formation in cells. After DNA damage, the distribution of

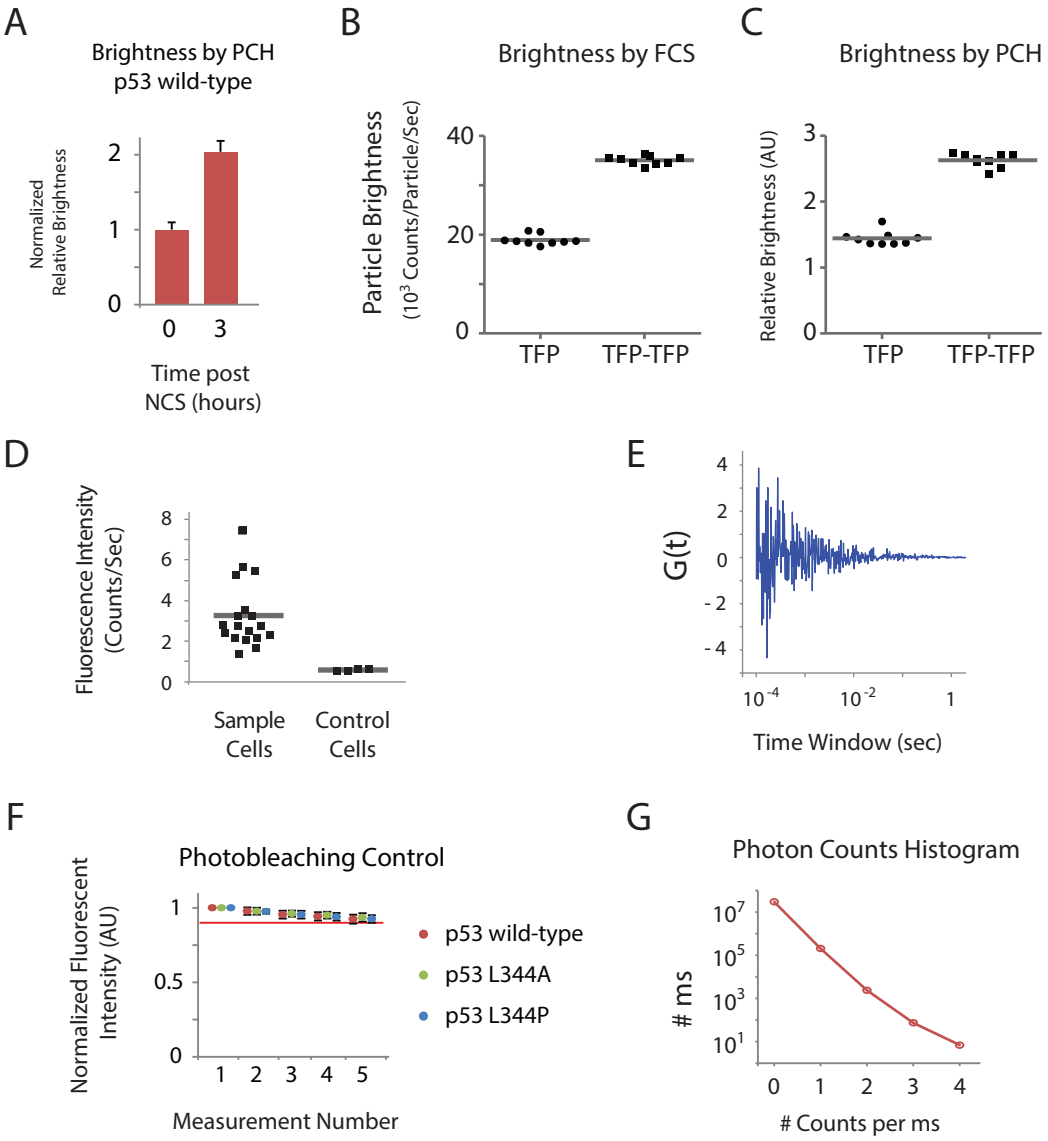
A
Brightness by PCH
p53 wild-type
Normalized
Relative Brightness
2
1
0
0
3
Time post
NCS (hours)
B
Brightness by FCS
Particle Brightness
(10³ Counts/Particle/Sec)
40
20
0
TFP
TFP-TFP
C
Brightness by PCH
Relative Brightness (AU)
3
2
1
0
TFP
TFP-TFP
D
Fluorescence Intensity
(Counts/Sec)
8
6
4
2
0
Sample
Cells
Control
Cells
E
G(t)
4
2
0
-2
-4
10⁻⁴
10⁻²
1
Time Window (sec)
F
Photobleaching Control
Normalized Fluorescent
Intensity (AU)
1
0.5
0
1 2 3 4 5
Measurement Number
p53 wild-type
p53 L344A
p53 L344P
G
Photon Counts Histogram
ms
10⁷
10⁵
10³
10¹
0 1 2 3 4
Counts per ms

Figure 2.3

Figure 2.3: Controls for the measurement of the brightness by FCS. A. The relative brightness of wild-type p53 calculated by photon counting histogram (PCH) technique at rest and 3 hours after DNA damage (mean +/- SEM, n = 5) shows the same behavior as the molecular brightness calculated by FCS (wt in Fig. 1C). **B-C.** Particle brightness of single TFP and tandem dimer TFP in cell lysates measured by FCS and PCH. Each dot corresponds to a fluorescent measurement and the grey line is the sample average. **D.** Comparison of fluorescence intensity of sample cells expression p53-mCerulean and control cells not expressing the fluorescent reporter (grey line represents the sample average). **E.** FCS analysis of two control cells not expressing the fluorescent reporter. The background signal does not show any autocorrelation. **F.** Photobleaching was minimal for all the cell lines used, expressing either p53 wild-type or p53 mutants L344A and L344P, in 5 consecutive measurements (mean and standard deviation, n = 25 for p53 wild-type, n = 20 for p53 L344A and n = 15 for p53 L344P). The red line represents the 0.9 intensity normalized by the first measurement. **G.** Photon counting distribution of a sample cell 3 hours after DNA damage with binning of 1 μs.

p53 stoichiometry drastically changed (Figure 2.2A and B): most p53 was bound in tetramers with only a small fraction of p53 dimers and monomers. This provides experimental evidence that DNA damage changes the balance of p53 oligomeric state in cells, pushing it toward higher order complexes.

2.2.2 After DNA damage p53 tetramerization precedes protein accumulation .

To capture the timing of oligomerization and the relationship with total p53 levels we induced DNA damage and followed both measures in individual cells over time. The total p53 protein (as reported by fluorescence intensity) slowly increases after damage due to stabilization of the protein rather than increased expression [98]. p53 oligomerization (reported by the particle brightness) increases more rapidly during the first 90 minutes, followed by a moderate continuous increase, suggesting that oligomerization precedes stabilization (Figure 2.4A and B). This order of events is clearly captured when plotting p53 oligomerization against total levels in each cell (Figure 2.4C).

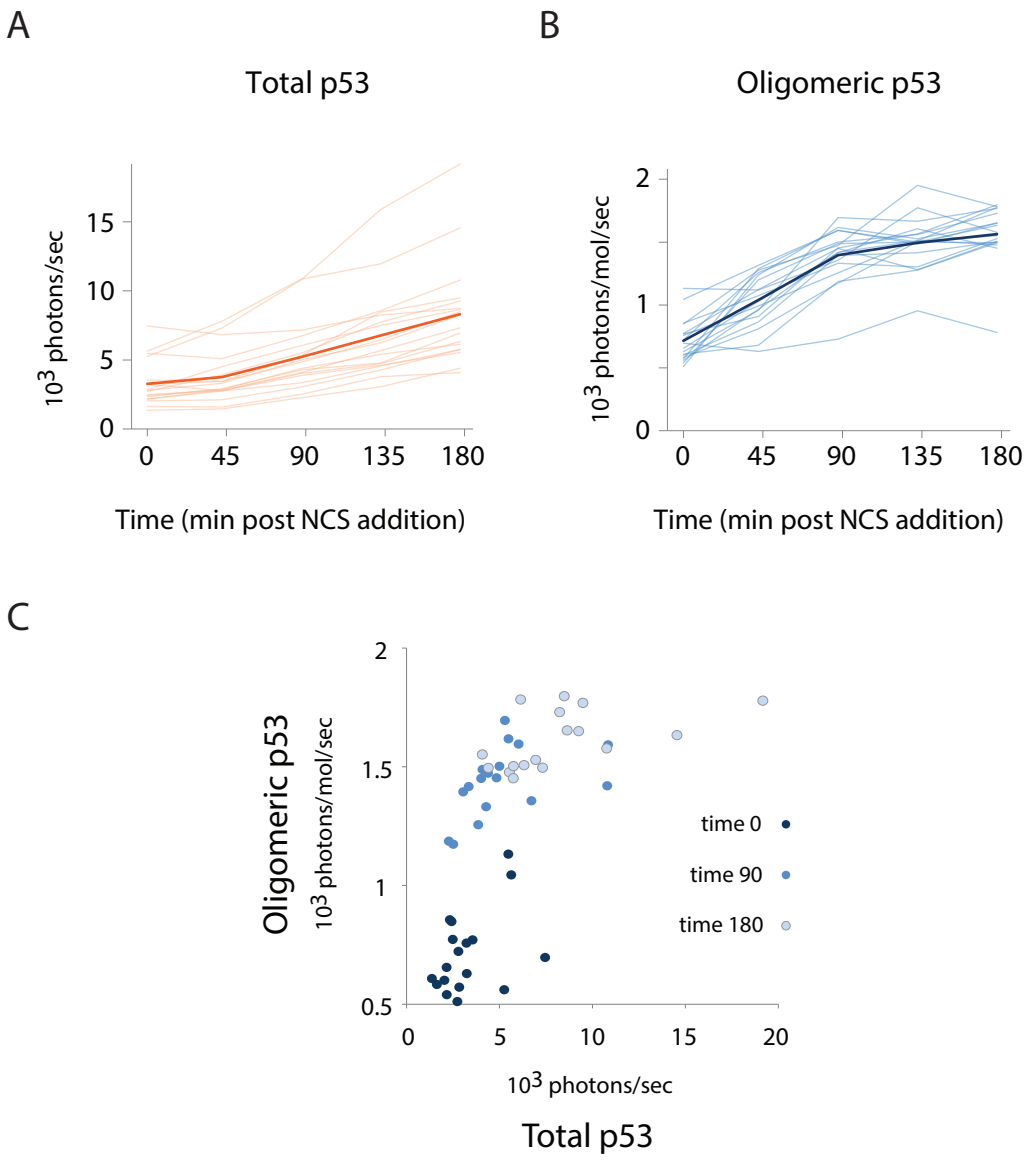

Figure 2.4: Dynamics of total and oligomeric p53 A. Dynamics of total p53 (orange lines) and **B.** dynamics of oligomeric p53 (blue lines) post DNA damage. Each trajectory is a single cell. The bold line is the average corresponding behavior. **C.** Scatter plot of data in panels A and B. Each dot is one single-cell measurement at the indicated time after DNA damage. Note that in the first 90 minutes after DNA damage, cells mainly move vertically in the scatter plot, indicating that oligomerization increases while total p53 does not change. In the following 90 minutes (180 min post damage) cells mostly move horizontally indicating that now the concentration of p53 increases with a minimal change in the oligomerization state.

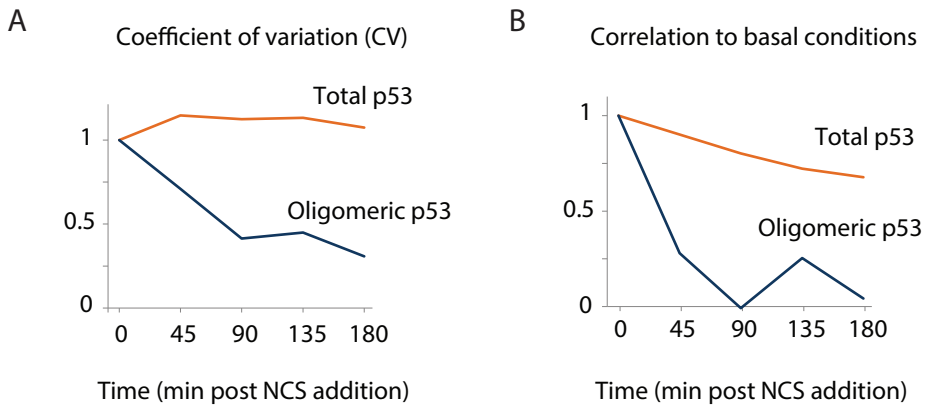

Figure 2.5: Correlation of total and oligomeric p53 during the time course. A. Cell-to-cell variation of total and oligomeric p53. Note that the coefficient of variation (CV) for total p53 does not change post damage, meaning that the variation between cells is constant. In contrast, the CV of oligomeric p53 decreases, denoting that cell-to-cell variation is reduced after DNA damage. **B.** The correlation between each time point post damage and basal conditions. Lower correlation values mean lower dependency between pre- and post DNA damage. The low correlation of oligomeric p53 by 90 min post damage indicates that all cells converge into a similar state independently of their initial state.

We observed two additional differences between the dynamics of p53 levels and the oligomeric state of p53 after DNA damage. First, the cell-to-cell variation in p53 total levels remains constant, while the variation in oligomeric state decreases with time after damage (Figure 2.5A). Second, the accumulation in p53 total levels after DNA damage was proportional to the basal level in each cell (Figure 2.5B), meaning that for the p53 protein levels the initial state of the cells affects its state 3 hours after damage. In contrast, by 90 minutes after DNA damage the extent of oligomerization was uncorrelated with the oligomeric states in basal conditions (Figure 2.5B). Taken together this suggests that cells with widely different oligomerization state converge to a common profile of predominantly tetrameric p53 (>90%, Figure 2.2B) following DNA damage.

2.2.3 Higher order p53 oligomers are degraded faster

What can explain the rapid tetramerization of p53 after DNA damaged followed by a delayed accumulation of the p53 protein? One possibility is that tetramerization itself is the mechanism through which the total p53 protein is stabilized. This would imply that the half-life of p53 tetramers should be higher than that of p53 dimers and monomers. We measured the half-life of p53 wild-type and the p53 mutants L344A and L344P in population and single cells (Figure 2.6). Surprisingly we found the opposite trend; monomeric p53 showed the longest half-life and wild-type p53 the shortest. Thus, the oligomerization of p53 does not contribute to the stabilization of the protein. The fact that total p53 increases despite the formation of less stable complexes appeared counterintuitive, and we therefore sought to develop a quantitative framework to explore the relationship between oligomerization and stabilization.

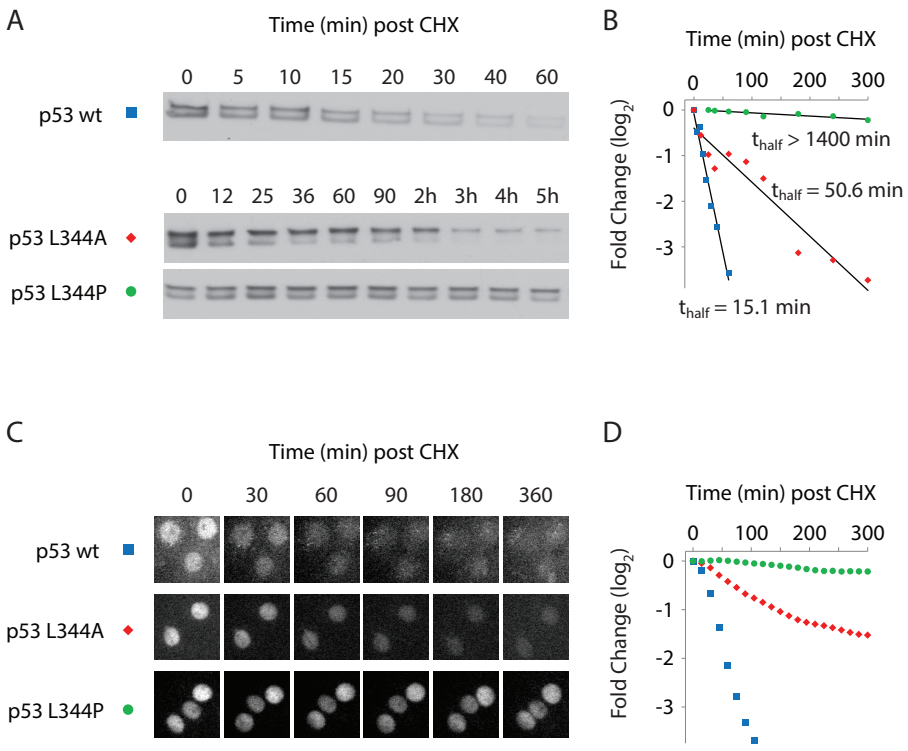

Figure 2.6: p53 tetramers are less stable than dimers and monomers. Cells expressing wild-type or mutated p53 were treated with 10 μg/mL cycloheximide and p53 levels were measured using immunoblots **A-B** and live cell imaging **C-D**. The p53 half-lives displayed in panel B were calculated by fitting a log-linear decay curve to the quantification of the blots.

2.2.4 The rapid surge of p53 tetramers requires active induction of tetramerization together with a decrease in degradation

We constructed a mathematical model including three species of p53, corresponding to the three possible oligomeric states (Figure 2.7A). Monomers of p53, M, are produced at a constant rate α and form dimers, D, and successively tetramers T. Each species is degraded at a different rate, β_m, β_d, and β_t, respectively. We used the data shown in Figures 2.1-2.6 to constrain the parameter values for cells at resting conditions (see Materials and Methods, Mathematical Modeling and Parameter Search section). We then modeled the effect of DNA damage on the system in several alternative ways and compared each output with the experimental data.

When we modeled DNA damage only as a decrease in p53 degradation by altering the values of β's, our model predicted a faster increase in total p53 levels than in its oligomeric state (Figure 2.7B). Such behavior was inconsistent with our experimental findings (Figure 2.4 and 2.7C). DNA damage modeled only as an induction of p53 tetramerization (by modifying k_{on}^{tet} and k_{off}^{tet}) led to a decrease in total p53 levels (Figure 2.7B), which also did not match the experimental data. Only when we modeled DNA damage as a combination of the two effects, decrease in degradation and induction of tetramerization, did the modeled dynamics agree with the measured dynamics (Figure 2.7B and C). Importantly the fast increase in oligomeric p53 in the model did not depend on the specific choice of parameters (Figure 2.8 and the Methods Section for model parameterization). We concluded that both induction of oligomerization and protein stabilization are required for the observed pattern of rapid surge of p53 oligomers after DNA damage followed by increase in total p53 levels.

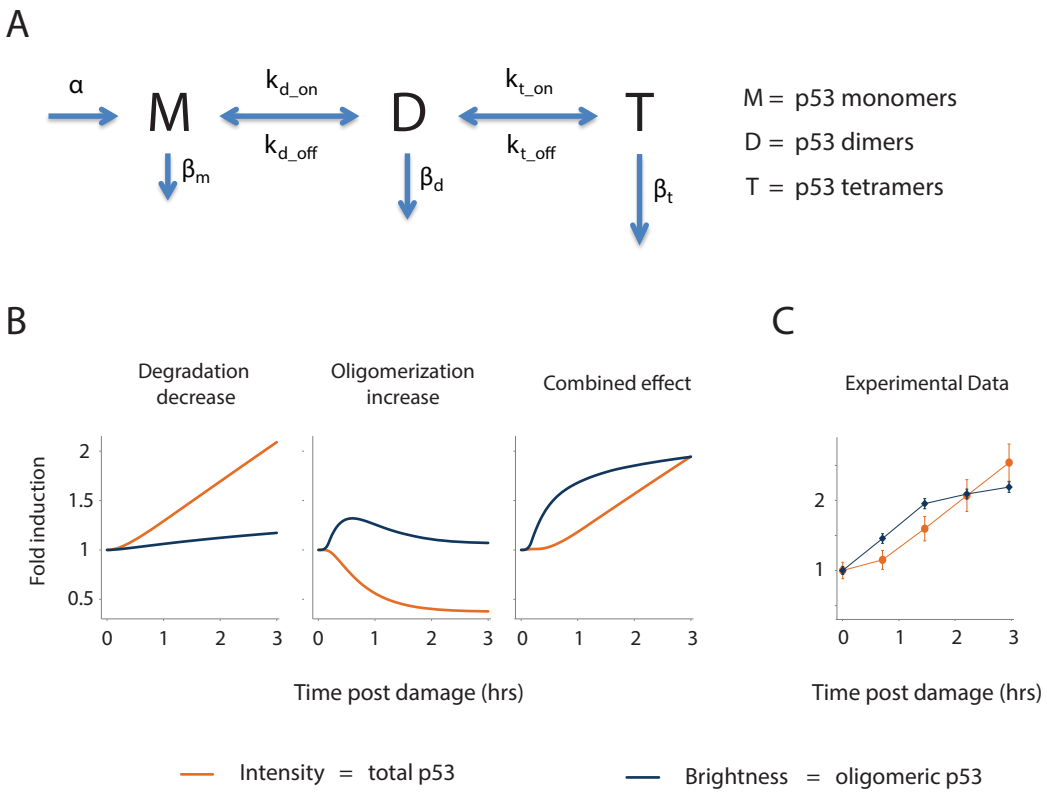

Figure 2.7: Mathematical model and simulation of p53 tetramerization and degradation. A. The model includes three species of p53: monomers M, dimers, D and tetramers T. p53 monomers are produced at rate α and molecules can bind and unbind to form homo-oligomers. Each oligomeric form of p53 can be degraded at rate β_i. **B.** Model simulation for the dynamics of total and oligomeric p53 after DNA damage, modeled in 3 ways: a decrease in p53 degradation (left panel), an increase in oligomerization (middle panel) or a combination of both effects (right panel). **C.** FCS Experimental data showing total and oligomeric p53 (mean and SEM, n = 18).

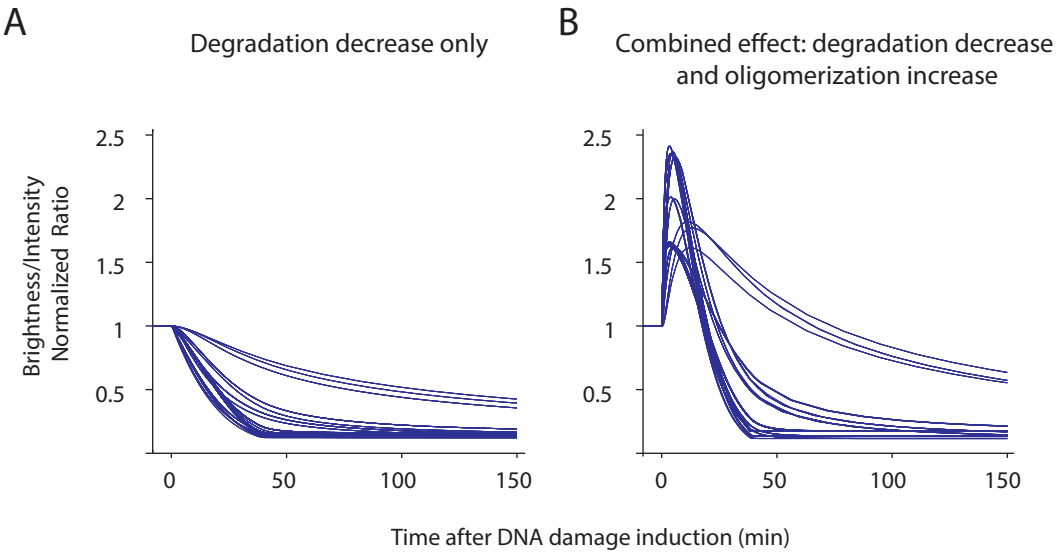

Figure 2.8: The requirement for DNA damage to induce oligomerization directly is independent of the parameter set chosen. The model was run for all the 349 parameter sets that match the experimental data at time 0. **A.** If DNA damage is modeled only as a reduction in p53 protein degradation, the ratio of particle brightness over total intensity remains below 1 independently of the parameters chosen. Hence oligomeric p53 cannot increase more than the total intensity. **B.** If DNA damage is modeled both as a reduction in p53 protein degradation and as an increase in p53 tetramerization, there is an initial window of time in which oligomeric p53 increases more than the total p53. This was the case for all the parameter sets tested.

2.2.5 Assembly of p53 tetramers does not require increase in concentration and is sufficient for activating p53 transcriptional targets.

Our result supports the existence of a mechanism induced by DNA damage that directly triggers p53 tetramerization independently of its total levels. p53 levels are primarily regulated by degradation, with new molecules constantly being made and degraded. We therefore asked whether tetramerization requires synthesis of new p53 molecules, or whether tetramers can be immediately assembled from existing molecules. Our model predicts that inhibition of protein synthesis in the absence of DNA damage should lead to a decrease in both p53 total level and oligomerization level (Figure 2.9A). After DNA damage is applied, total p53 protein should keep decreasing while the levels of tetrameric p53 should increase. Our experimental FCS measurements matched these predictions; oligomeric p53 increased after DNA damage even when synthesis was inhibited. We therefore conclude that existing molecules of p53 can be assembled into tetramers.

Is the assembly of p53 tetramers sufficient to induce p53 transcriptional activity? This was previously impossible to determine since the extent of tetramerization in cells was unknown and tetramer formation was thought to be a direct result of the increase in total p53 concentration. Since we can now separate the increase in total p53 levels from the increase in p53 tetramers (Figure 2.9B), we can assess the effect of tetramerization on p53 transcriptional activity independent of the increase in its total level. We observed that p53 targets were induced after DNA damage even when p53 levels decreased (Figure 2.9C). Such induction was not observed when we used a cell line expressing the oligomerization mutant p53 L344A, which forms dimers but not tetramers. These results suggest that tetramerization of p53 is sufficient to activate transcription, without an increase in total p53 protein.

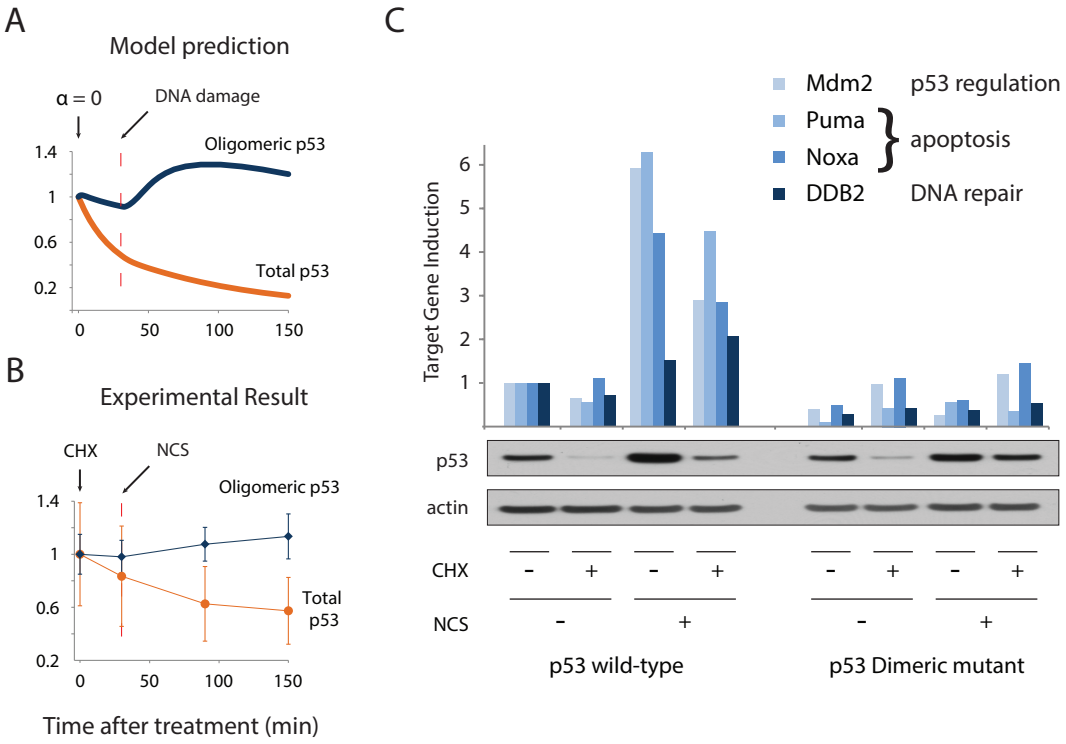

Figure 2.9: p53 tetramerization is sufficient for triggering target gene activation without an increase in p53 levels. **A.** Model simulation of total (orange line) and oligomeric (blue line) p53 after translation inhibition (t = 0), followed by DNA damage. **B.** Experimental confirmation of the model simulation (mean and standard error, n=6). **C.** p53 transcriptional targets were measured using qPCR in response to DNA damage (NCS) and translation inhibition (CHX) for both wild-type p53 and dimeric mutant p53 L344A. Combination of CHX and NCS leads to an increase in the expression of p53 target genes even when p53 levels are not induced. Induction of p53 target genes is not seen under these conditions for the p53 L344A mutant that can form dimers but not tetramers, suggesting that the induction of p53 targets depends on p53 ability to tetramerize.

2.3 CONCLUSIONS

Our results indicate that p53 homo-oligomerization in cells is a highly regulated process. The balance between monomers, dimers and tetramers is not simply determined by the concentration of p53 molecules. Stress responses, such DNA damage, can trigger p53 tetramerization even when the protein concentration does not increase.

Our study highlights the importance of studying protein homo-oligomerization in cells, where the effects of post-translational modifications and co-factors modulating oligomerization can be evaluated. Several co-factors have already been shown to regulate p53 oligomerization *in vitro*. For example, S100 proteins were shown to preferentially bind p53 monomers and inhibit oligomerization [99], and p53 phosphorylation was shown to decrease its tetrameric K_d through binding with 14-3-3σ [57]. In addition, p53 binding to specific DNA was suggested to enhance tetramerization [56]. Therefore, modifications that increase p53 binding to DNA could have an indirect effect on the oligomerization state of p53. However even the effects of the known co-factors on the *in vitro* K_d for p53 tetramerization cannot explain the extent of tetramer concentrations we observed in cells following DNA damage, suggesting the existence of additional unknown regulators of p53 oligomerization. Since our results demonstrate that p53's activity as a transcription factor can be triggered by induction of tetramerization, identification of these unknown factors may point to new targets for modulating p53's function in cancer. The approach we used here should be of general utility in studying the quantitative dynamics and function of oligomerization of transcription factors and other proteins in any cellular system [100].

2.4 Materials and Methods

Cell line construction

The cell line MCF7+p53shRNA was kindly provided by Reuven Agami group [97], Netherlands Cancer Institute, Amsterdam, Netherlands. cDNA for p53 was altered by site-directed mutagenesis (QuikChange kit, Stratagene) at residue 344 to obtain oligomerization mutants p53 L344A and p53 L344P, and with 7 silent point mutations that allow for mRNA to escape shRNA silencing without altering the amino acid sequence. p53 was expressed under the EF1α promoter and tagged with mCerulean. The vector was introduced in cells via lentiviral infection and stable clonal selection. Lentiviral particles were produced in 293T cells. The fluorescent protein mCerulean has maturation time comparable to Venus [101] which matures in less than 10 minutes at 37 Celsius degrees [102].

Cell culture, DNA damage, and cycloheximide treatment

MCF7+p53shRNA+p53-mCerulean cells were maintained in RPMI supplemented with 10% fetal calf serum, 100 U/ml penicillin, 100 mg/ml streptomycin, 250 ng/ml fungizone (Gemini Bio-Products) supplemented with selective antibiotics (400 μg/ml G418 and 0.5 μg/ml puromycin). DNA damage was induced by neocarzinostatin (NCS, Sigma) at 400 ng/mL final concentration. Translation inhibition was induced by cycloheximide (Sigma) at final concentrations of 10 μg/mL for Figure 2.6 and 1μg/mL for Figure 2.9. Cells were harvested for protein/RNA extraction at the indicated times after DNA damage and/or translation inhibition.

Western Blot Analysis

Harvested cells were lysed in the presence of protease and deacetylase inhibitors. Total protein levels were quantified using the BCA assay (Pierce). Equal protein

amounts were separated by electrophoreses on 4%–12% Bis-Tris gradient gels (Invitrogen) and transferred to PVDF membranes by electroblotting. Membranes were blocked with 5% nonfat dried milk, incubated overnight with primary antibody, washed, incubated with secondary antibody coupled to peroxidase. Protein levels were detected with chemoluminiscence (ECL plus, Amersham). p53 dynamics were quantified by normalizing total p53 levels (DO1, Santa Cruz) to α-actin (Sigma).

Target gene expression dynamics

Total RNA was extracted using the RNeasy protocol (Qiagen). RNA concentration was determined by measuring absorbance at 260 nm. Equal RNA levels were used to generate complementary DNA using the high-capacity cDNA reverse transcription protocol (Applied Biosystems). Quantitative PCR was performed using reaction mixtures of 8.4 ng total RNA, 100 nM primer, and SYBR Green reagent (Applied Biosystems).

FCS measurements and analysis

Two days before microscopy, cells were grown on poly-D-lysinecoated gridded glass-bottom plates (MatTek Corporation). Multiphoton FCS was carried out on a custom built setup based on a Nikon TE2000 microscope. For ECFP excitation, a collimated 850nm IR laser beam (Mai Tai, Ti:Sapphire laser with 80MHz and 100 fs pulse width, Spectra-Physics, CA, USA) was aligned into Nikon 100X Plan Apochromat oil immersion objective (N.A.=1.4) with back aperture slightly overfilled, creating a diffraction-limited focal spot. The laser power was controlled below 2 mW to avoid photobleaching of the fusion protein, cellular photodamage and DNA damage. The collected fluorescence was passed through band-pass filters (HQ485/70m-2p for Cerulean (Chroma Tech) and focused onto a photomultiplier

tube (H7421, Hamamatsu, Japan). The cells were maintained in an aluminum chamber [103] with temperature-controlled water circulation system set to 37 Celsius degree. Each autocorrelation curve measured in nucleus were collected for 30 seconds using Flex02-01D/C correlator (correlator.com) and transferred to a personal computer through a high speed USB port. The PMT dead time is 70ns and the correlator dead time is 1.56ns. The frequency of photon counts was always less than 20 kHz, corresponding to a flow of $2x10^{-5}$ photon counts per nano-second, far from the saturation intensity – see sample histogram of photon counts distribution in Figure 2.3G. For average purpose, five FCS curves were recorded at each position in single cell at each time point buffering non-recurrent kinetics such as the ones caused by extremely slow moving particles. All FCS curves were analyzed by custom-written Matlab code (Mathworks Inc, Waltham, MA) using a nonlinear least-squares fitting algorithm from the curve fitting toolbox (2011). The fitting formula for single-component diffusion is adapted from [104]:

$$G(t) = \frac{1}{<N>}(1 + \frac{t}{\tau_D})^{-1}(1 + \frac{t}{\omega^2\tau_D})^{-\frac{1}{2}},$$

where <N> is the average particle number of species in the sampling volume. τ_D is the residence time of species within the sampling volume, with $\tau_D = \omega^2 \frac{xy}{8D}$, where D is the diffusion coefficient of the species, and $\omega = \frac{\omega z}{\omega xy}$ is the aspect ratio of the sampling volume. Before the fit analysis, raw FCS autocorrelation curves were denoised by averaging the five curves. Each averaged FCS curve was fitted by the formula above to get the diffusion property, molecule number. The brightness ε was calculated as

$$\varepsilon =< I > *G(0) = \frac{<I>}{<N>}$$

Notably, the diffusion coefficient changed minimally over the course of the ex-

periments (Figure 2.2C), and hence the molecular residence time was constant, indicating that the particle brightness analysis is appropriate in this context [96]. Moreover, other proteins that bind p53 could change the diffusion coefficient D; however since G(0) is independent of D, such binding will not affect the calculated brightness.

FCS brightness validation measurement in cell lysates

The acquired plasmid pmTFP was cut out and inserted into a EYFP-C1 vector by NheI/BglII to form pmTFP-C1 vector. Tandem TFP-TFP plasmid was generated by inserting a TFP ORF generated by PCR into the pmTFP-C1 vector by Sal1/Mfe1 into Xho1/Mfe1. 293T (human embryonic kidney) cells were seeded into 10 cm petri dish and antibiotics were removed one day before the transfection. Transient transfection of TFP and TFP-TFP plasmid into 293T cell was carried out using Lipofectamine LTX and PLUS reagents (Invitrogen). Total 10 μg DNA plasmid was added with Opti-MEM media with LTX and PLUS to cells at 50% confluence. Cells were harvested one day after transfection, pelleted and resuspended in 100 μl lysate buffer (20mM HEPES, 5mM KCl, 1.5mM MgCl2 and protease inhibitors (Roche)). The lysate incubated on ice for 30 minutes followed by centrifuge at 14k rpm 4C for 30minutes. The supernatant was further centrifuged at 40k rpm 4C for 30 minutes. The collected supernatant was diluted in lysate buffer for FCS measurement. The laser power was set to 10mw, a level at which no photobleaching was observed.

Time-lapse Microscopy

Two days before microscopy, cells were grown on poly-D-lysinecoated glass-bottom plates (MatTek Corporation) in transparent medium supplemented with 5% fetal calf serum, 100 U/ml penicillin, 100 μg/ml streptomycin, and 250 ng/ml fungizone (Gemini Bio-Products). Cells were imaged with a Nikon Eclipse Ti-inverted

Table 2.1: Mathematical model equations. Ordinary differential equations used to model the dynamics of p53 oligomerization, from monomeric p53 (M) to dimeric (D) and tetrameric p53 (T). A full description of the parameters is given in Table S2.

Variable	Differential Equations
M = monomers of p53	$\frac{dM}{dt} = a - 2k_{on}^{dim} * M^2 + 2k_{off}^{dim} * D - b_m * M$
D = dimers of p53	$\frac{dD}{dt} = k_{on}^{dim} * M^2 - k_{off}^{dim} * D - 2k_{on}^{tet} * D^2 + 2k_{off}^{tet} * T - b_d * D$
T = tetramers of p53	$\frac{dT}{dt} = k_{on}^{tet} * D^2 - k_{off}^{tet} * T - b_t * T$

fluorescence microscope on which the stage was surrounded by an enclosure to maintain constant temperature, CO^2 concentration, and humidity. Images were acquired every 15 min. The CFP filter set was 436/20nm excitation, 455nm dichroic beam splitter, and 480/40nm emission (Chroma). We analyzed images using MetaMorph software (Molecular Devices) and custom written MATLAB software (Mathworks), which is available upon request.

Mathematical Modeling and Parameter search

The model for p53 oligomerization consists of three ordinary differential equations, Table 2.1, with 8 parameters listed in Table 2.2. Because of the lack of experimental techniques capable of measuring tetramerization *in vivo*, most of the parameters of the model are not available in the literature. Table 2.3 includes a list of relevant biophysical measurements available in the literature or measured in this work.

Our goal is to identify a global pattern of behavior independent of parameter sets. The model is therefore non-dimensional, meaning that the variables and the parameter values are unit-less. Comparison of model parameters to known experimental values (Table 2.3) would require defining scales for concentration and time, arbitrarily chosen and potentially misleading. Furthermore a fitting procedure could have provided us with the parameter sets that best described the data.

Table 2.2: Parameters of the mathematical model. In the initial analysis all parameters were allowed to span a range of 7 orders of magnitude. The choice of parameters is described in the Materials and Methods section.

Parameter symbol	Description
a	production rate of p53 molecules
k_{on}^{dim}	dimerization reaction on-rate
k_{off}^{dim}	dimerization reaction off-rate
k_{on}^{tet}	tetramerization reaction on-rate
k_{off}^{tet}	tetramerization reaction off-rate
b_m	monomeric p53 degradation rate
b_d	dimeric p53 degradation rate
b_t	tetrameric p53 degradation rate

However we decided against fitting our model to the data because the degrees of freedom of the parameters outweighed the constraints our data could pose on them. This would result in multiple solutions for the parameter space without a clear way of testing which solution would be more appropriate.

Instead we kept the values of each parameter equal to a power of 10, i.e. having every step change in parameter correspond to one order of magnitude. We then used the data collected from the FCS measurement on the cell line expressing p53wt-mCerulean before stress as described below:

1. we first allowed each parameter to attain the each of 7 possible parameter values, 10^i, where i= -3,-2,-1,0,+1,+2,+3, spanning 7 orders of magnitude; this created a combinatorial set of over 5 million possible parameter sets,

2. we derived analytically the steady state solutions of the ODE's in Table 2.1 and we calculated the steady state values for the 3 species of p53 for each parameter set,

3. we narrowed down the plausible parameters sets using 3 measurements:

    a) the brightness of wild-type p53 at time 0, from Figure 2.2A, +/- 5%

    b) the Dimer/Monomers and Tetramers/Monomers ratios, from Figure 2.2B +/- 50%

    c) requiring that $\beta_t > \beta_d > \beta_m$ from Figure 2.6.

Using these criteria we narrowed down the parameter space to 349 sets. Figure 2.8 shows that a combined effect, of both degradation decrease and oligomerization increase, is required to match the trend in the experimental evidence (Figure 2.7C) independent of parameter values.

Table 2.3: Experimentally tested parameters. Table of biophysical experimental measurements and their corresponding model parameters.

Physical Parameter	Description	Model Parameter	Value	Source
K_d Mono-Dim	Dissociation constant of dimerization reaction	$k_{off}^{dim}/k_{on}^{dim}$	~ 0.55 nM	[53]
K_d Dim-Tet	Dissociation constant of tetramerization reaction	$k_{off}^{tet}/k_{on}^{tet}$	100nM - 1μM	[57][56]
t_{half} monomer	Half-life of monomeric p53	$1/b_m$	~1000 min	Figure 2.6

To model the perturbations caused by DNA damage we modified the corresponding parameters: b_m, b_d and b_t for changes in degradation, k_{on}^{tet} and k_{off}^{tet} for changes in the tetramerization reaction. We attempted both step changes, linear and exponential decays for both reduction in degradation and the stabilization of tetramerization. Qualitatively the main conclusion from the model holds true under all types of perturbations of the model we tested, clearly with quantitative differences in overall timescale of simulation and magnitude of total p53 increase (in fact as Figure 2.8 shows even with the same type of perturbation, different parameter sets have faster dynamics than others). For Figure 2.7 and Figure 2.8 the degradation decay is simulated as an exponential decay. The degradation rates of all three species of p53 (monomeric, dimeric and tetrameric) were lowered by the same proportion, hence keeping the ratios between degradation constants the same as before damage. The stabilization of tetramerization is modeled as a linear decrease in tetramerization off-rate and linear increase in tetramerization on-rate.

2.5 Author Contributions

This Chapter is adapted from Gaglia et al, 2013 work was published as

> Giorgio Gaglia, Yinghua Guan, Jagesh V. Shav & Galit Lahav, Activation and control of p53 tetramerization in individual living cells. *PNAS*, vol 110, no. 38, pp. 15 497-501, 2013.

Author contributions: Giorgio Gaglia, Jagesh V. Shah and Galit Lahav designed the research. Yinghua Guan contributed new reagents and analytic tools. Giorgio Gaglia conducted the experiments and performed the analysis, with help from co-authors. In particular the FCS experiments were conducted by Giorgio Gaglia and Yinghua Guan. Giorgio Gaglia and Galit Lahav wrote the paper.

This page intentionally left blank.

Chapter 3 : A molecular throttle maintains constant rate of p53 tetramerization in response to DNA damage

The dynamics of the tumor suppressor protein p53 have been previously investigated in single cells using fluorescently tagged p53. Such an approach reports on the total abundance of p53 but does not provide a measure for functional p53. We used bimolecular fluorescence complementation to quantify in single cells the dynamics of p53 tetramers, the functional units of p53. We found that while total p53 increases proportionally to the input strength, p53 tetramers are formed in cells at a constant rate. This breaks the linear input-output relation and dampens the p53 response. Disruption of the p53-binding protein ARC led to a dose-dependent rate of tetramers formation, resulting in enhanced tetramerization and induction of p53 target genes. Our work suggests that constraining the p53 response in face of variable inputs may protect cells from committing to terminal outcomes and highlights the importance of quantifying the active form of signaling molecules in single cells.

3.1 INTRODUCTION

Biological systems often exhibit a graded response in which the stronger the input the higher and broader the output. However, in some systems the output is constrained through feed-forward motifs or feedback loops, buffering against fluctuations or extreme signals [105, 106, 107]. Restriction of the output can also be achieved by a rate limiting activator not affected by the input ("A" in Figure 3.1). Alternatively constant activation in face of variable input strengths can result from an inhibitory mechanism. In this scenario the activation is constrained by a tunable valve, the function of which increases with the input strength ("I" in Figure 3.1). Such a mechanism, referred to as a throttle, is commonly used in engineering. In order to identify and characterize such potential mechanisms in biology we need to be able to accurately measure both the total level of a signaling protein and its active form in the same cell in response to variable input strength. Here we quantified the total protein level of the tumor suppressor p53 and its active tetrameric form in single cells in response to a range of UV doses, and identified a throttling mechanism for damping p53 activity at high UV levels.

The p53 protein is induced in response to stress and triggers different cellular outcomes including cell cycle arrest, apoptosis and senescence [108]. Fluorescence reporters of p53 have previously been used to study the dynamics of p53 in live cells [32, 35, 36]. These studies revealed that p53 dynamics depend on the stimulus and carry information that determines cellular outcomes. UV radiation for example, leads to a transient increase in p53 protein level displaying a single graded pulse. The amplitude and duration of the pulse depend on the UV dose, with higher doses leading to stronger and longer p53 induction [33] and to cell death [22]. However, fluorescently tagged p53 reports only for the dynamics of total p53,

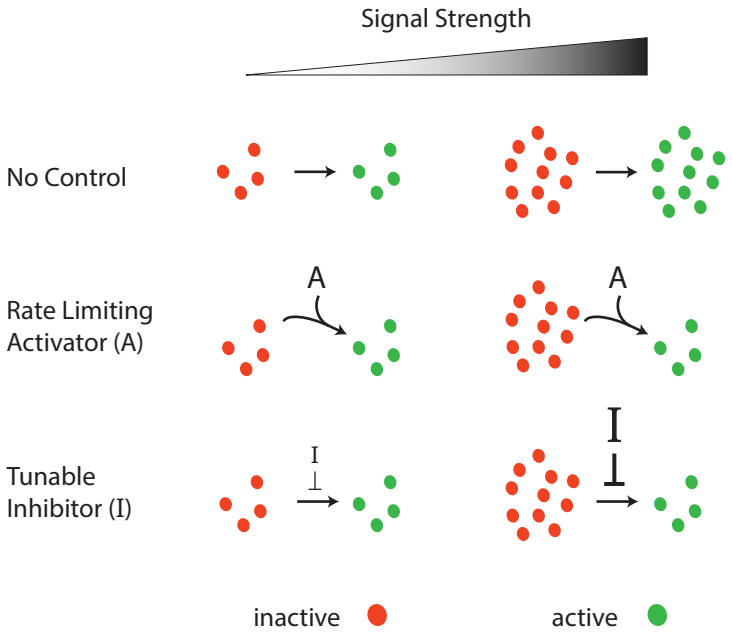

Figure 3.1: Signalling control strategies. Schematic drawing of potential mechanisms constraining the levels of an active molecule. In all cases, the levels of an inactive molecule (red) are proportional to the signal strength. In the absence of a control system (top) the levels of the active form (green) are also proportional to the signal strength. The linear relationship between signal strength and molecule activation can be broken either by the presence of a constant activator "A", which limits the rate of activation (middle) or by the presence of a tunable inhibitor "I" the strength of which depends on the strength of the signal (bottom).

and does not capture the dynamics of active p53, which depends on specific modifications and homo-oligomerization.

Activity of transcription factors in single cells can be quantified using various methods. In cases where the transcription factor is regulated through localization fluorescent tagging was used to report for transcriptional activity [109, 110]. p53 is stably localized in the nucleus and therefore localization is not a sufficient measure for its activity. Transcription factors' activity in cells can also be measured by a transcriptional reporter, in which a target gene promoter drives the expression of a fluorescent protein. Such an approach has been used, for example, to study the activity of the circadian clock gene Per1 [111] and the dynamics of ComK, the 'master' transcription factor of genes necessary for competence in Bacillus subtilis [112]. In the p53 pathway different target genes show different patterns of activation, implying that their induction depends on additional factors beyond p53 and making it impossible to choose a single promoter as a general readout for p53 activity [22].

Tetramerization of p53 has been shown to be fundamental for its ability to bind DNA and activate transcription, suggesting tetramerization as a valuable measure for globally quantifying the functional unit of p53 in single cells. The formation of p53 tetramers is driven by a C-terminal tetramerization domain. The reaction proceeds in two steps: first p53 monomers bind into dimers, which then form tetramers. Importantly the tetrameric binding interface only forms when dimerization has occurred, hence p53 tetramers are referred to as "dimers of dimers". Previous *in vitro* work showed that p53 dimerization occurs co-translationally, on the polysome, suggesting that p53 dimers are composed of monomers translated from the same mRNA [55]. Furthermore p53 was suggested to be primarily dimeric in cells, as the dimer dissociation constant is in the order of 10^{-4} µM [53, 56], several orders of magnitude lower than p53 cellular concentration (~0.1-10µM). Tetramer-

ization occurs post-translationally with a much higher K_d of ~1μM, which can be altered by post-translational modifications and co-factor binding [67, 57, 94]. Mutations in the p53 tetramerization domain (326-356 aa) lead to a reduction in, or loss of, its transcriptional activity in cells [68] and were shown to cause early cancer onset, known as Li-Fraumeni syndrome [70, 74].

In Chapter 2 we used fluorescence correlation spectroscopy (FCS) to measure the tetramerization of p53 in single cells [113]. This method allowed quantifying the stoichiometry of p53 oligomers directly in live cells and monitoring their temporal changes after DNA damage. However, FCS is a low-throughput method; the number of cells measurable by FCS is limited (~5-20) and the single cell dynamics can currently only be measured manually. Here we developed a bimolecular fluorescence complementation (BiFC) assay to quantify the dynamics of p53 tetramers in single cells and investigated how cells regulate total p53 and its activity under various input strength.

3.2 Results

3.2.1 BiFC captures p53 tetramerization in single cells

To investigate the dynamics of p53 oligomerization in cells we used bimolecular fluorescence complementation (BiFC). BiFC relies on splitting a fluorescent protein in two complementary fragments, and tagging each to one of two proteins that potentially bind each other. The split fragments are not fluorescent alone and bind each other with low affinity. When they are brought together by the stable interaction of the proteins they are tagged to, the full fluorescent protein is able to form leading to a fluorescent signal (Figure 3.2A and [90, 91, 114]).

We tagged two copies of p53 to two different halves of YFP (YFP-N or YFP-C) and stably expressed them in human cells. Each p53 was also tagged to a full-

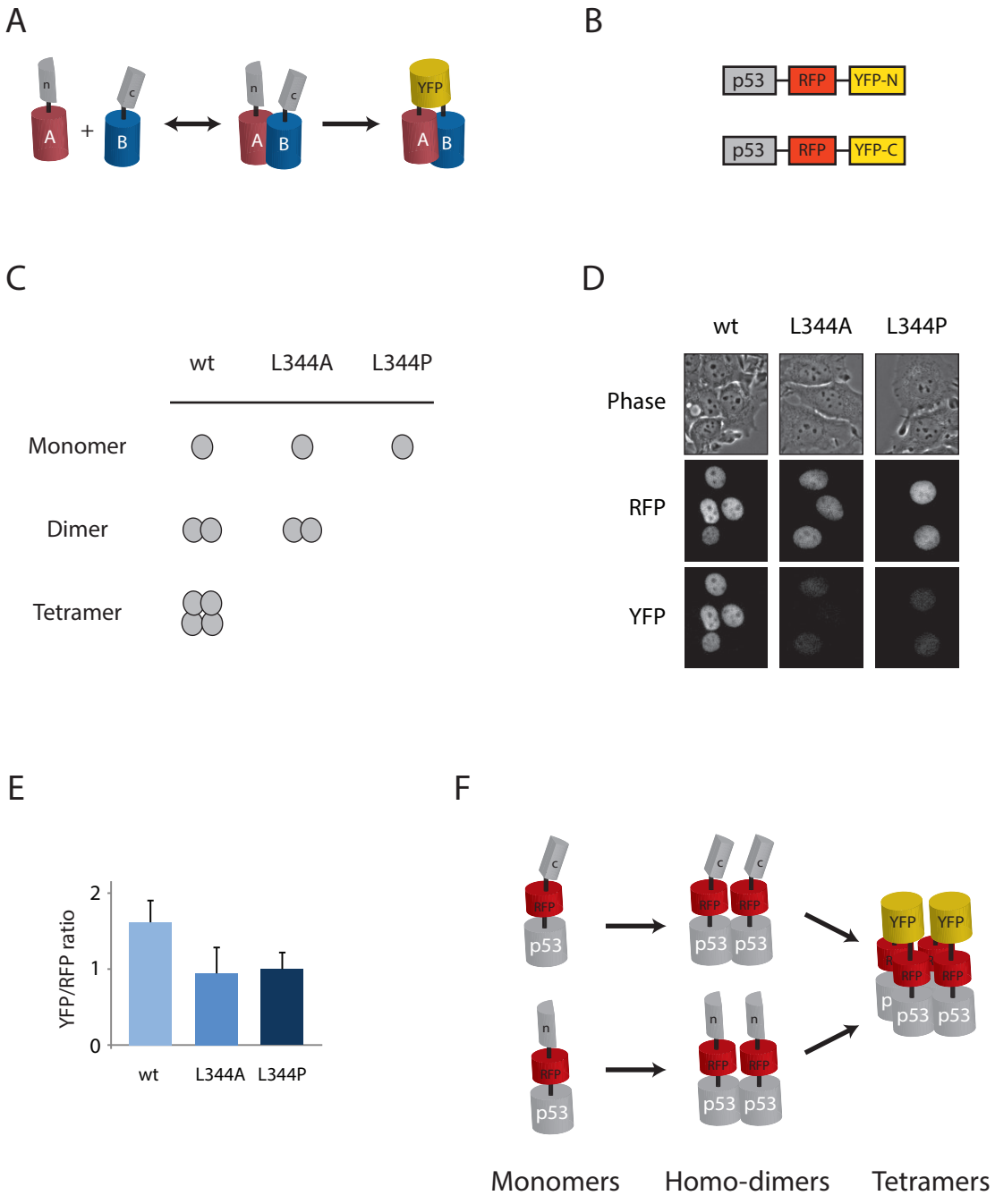
A
n
c
A
B
+
YFP
B
p53
RFP
YFP-N
p53
RFP
YFP-C
C
wt
L344A
L344P
Monomer
Dimer
Tetramer
D
wt
L344A
L344P
Phase
RFP
YFP
E
YFP/RFP ratio
2
1
0
wt
L344A
L344P
F
RFP
p53
YFP
Monomers
Homo-dimers
Tetramers

Figure 3.2

Figure 3.2: BiFC reports for p53 tetramerization A. BiFC is based on tagging putative interactive proteins ("A" and "B") with two different fragments of a fluorescence protein ("n" and "c"). The interaction between A and B brings the non-fluorescent fragments in close proximity and they form a full fluorescent protein. **B.** Schematic drawing of the p53 reporters. **C.** Schematic drawing of the various p53 species; p53 L344A forms dimers but not tetramers while p53 L344P is fully monomeric, since it is not able to form dimers or tetramers. **D.** Images of cells expressing the constructs in panel B with mutant or wild-type p53 in bright-field illumination, RFP and YFP. All cells show the RFP signal (total p53), but only the cells expressing wild-type p53 show YFP signal (p53 tetramers). **E.** Ratio of YFP to RFP fluorescence level in cells. Mean and standard deviation are reported and values are normalized to p53 L344P sample. N > 50 for each condition. **F.** p53 forms homo-dimers, in which both monomers are tagged with the same fragment of YFP leading to no YFP signal. When two dimers form tetramers the split YFP protein is formed and becomes fluorescent.

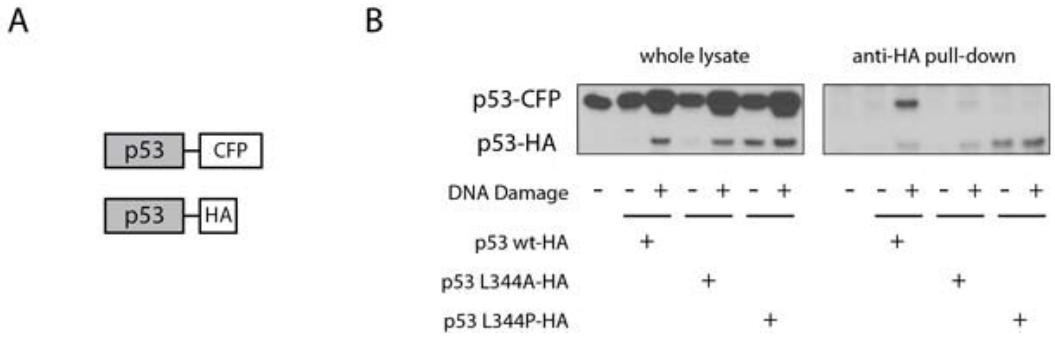

Figure 3.3: Co-immunoprecipitation of biochemically tagged p53. A. p53 was tagged with biochemical tags HA and CFP and expressed in cells. **B.** Co-immunoprecipitation experiment in cells expressing wild-type p53-CFP together with either mutant or wild-type p53-HA. Cells were damaged with the radiomimetic drug NCS and lysates were collected 2.5 hours after treatment. When wild-type p53-HA is pulled-down, p53-CFP co-precipitates, indicating that hetero-oligomers are formed. When the "dimers only" mutant p53 (L344A-HA) or fully monomeric mutant p53 (L344P-HA) are expressed and pulled down, p53-CFP does not co-precipitate, indicating that no heterodimers are present in cells.

length red fluorescence protein (RFP) to report for the total p53 protein in cells (Figure 3.2B). In principle, the formation of both p53 dimers and tetramers could yield fluorescence. In order to separate the contribution of each of these states to our measurements we used two well-characterized mutants of p53; p53 L344A that forms dimers but not tetramers, and p53 L344P, which is exclusively monomeric (Figure 3.2C). As expected, the p53 L344P monomeric mutant showed extremely low YFP signal (Figure 3.2D), representing auto-fluorescence or unspecific binding between the YFP fragments. Notably, the p53 L344A mutant that is able to form dimers did not display higher YFP fluorescence than the monomeric mutant (Figure 3.2D). Accordingly the ratio between the YFP signal to total p53 (measured by the RFP signal) in the L334A mutant was equivalent to the ratio obtained from the monomeric mutant L334P (Figure 3.2E), confirming that dimerization of p53 does not add fluorescence signal beyond the background observed by the monomeric p53. This suggests that p53 dimers are homo-dimers, meaning every dimer comprises the same two halves of YFP (Figure 3.2F). This is in agreement with recent in-vitro studies showing that p53 dimers are formed co-translationally, consisting of two monomers translated from the same mRNA [55]. Once formed the dimers' low dissociation rate and the short half-life of p53 keeps dimers from exchanging monomers.

We further confirmed the homo-dimerization of p53 by a pull-down assay of cells expressing two p53s fused to HA or CFP (Figure 3.3). This biochemical assay confirmed that in cells p53 dimers are indeed homo-dimers and that hetero-oligomers are formed only at the level of tetramers. The lack of p53 hetero-dimers and the increased YFP signal obtained from wild-type p53 (Figure 3.2D and E) indicates that the BiFC experimental setup is suitable for quantifying the level of p53 tetramerization in single cells (Figure 3.2F).

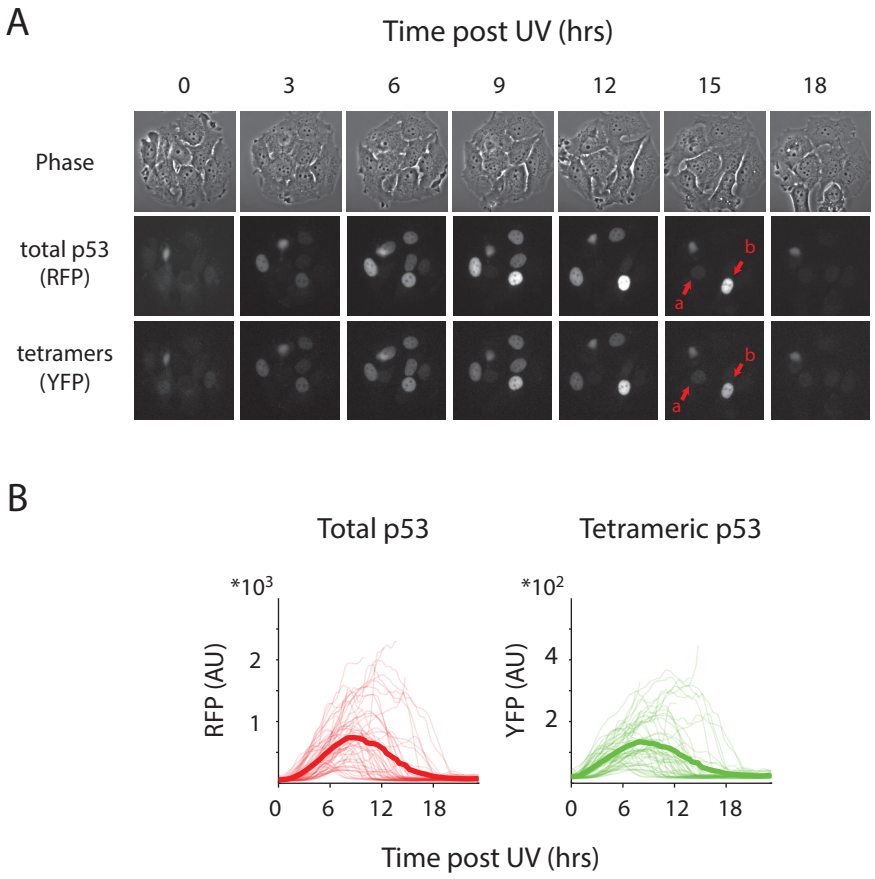

Figure 3.4: Time lapse images and quantification of total and tetrameric p53 after UV. A. Sample time lapse images of a field of cells following 6 J/m^2 UV. **B.** Quantification of nuclear fluoresence in single cells after 6 J/m^2 UV. Each trace is a single cell. Bold traces represent the mean dynamics (n = 100).

3.2.2 Formation of p53 tetramers is damped at increasing UV doses

Images of cells expressing the p53 tetramer reporter revealed that UV irradiation triggers a transient single pulse of p53 tetramers, similar to the dynamics observed for total p53 (Figure 3.4). However, when we treated cells with a range of UV doses we observed a major difference between the dynamics of total p53 and tetrameric p53. Higher doses of UV led to an increase in the amount of total p53 as was previously reported [33]. p53 tetramers also showed higher levels with higher UV doses, however the effect was limited in comparison to total p53 (Figure 3.5A). Quantitatively, the ratio between p53 tetramers and total p53 decreases with higher levels of UV, indicating damping of p53 tetramers (Figure 3.5B). To quantify the damping in single cells we plotted the peak levels of total and tetrameric p53 in each cell (Figure 3.5C). At a low UV dose (3 J/m^2) the peak levels were linearly correlated (red line). If tetramerization follows total p53 levels linearly, one would expect both the RFP and YFP signal to increase proportionally and to follow the red line under various UV doses. Instead, at a high UV dose (12 J/m^2) cells shifted to the right of the red line in the scatter plot, indicating that the increase in tetramerization does not match the increase in total p53.

3.2.3 p53 tetramers are formed at a constant rate independent of input strength

We next asked what leads to the damping of p53 tetramers in response to high levels of UV. The dynamics of p53 post UV can be described by two main properties: the rise time, which is the duration of the increase; and the slope, which is the rate at which the signal accumulates (Figure 3.6A). The damping in the ratio between p53 tetramers and total p53 could derive from modulation of either of these two properties. We found that the rise time increases with higher UV doses for both total p53 and p53 tetramers (Figure 3.6B). Damping in p53 tetramers therefore cannot

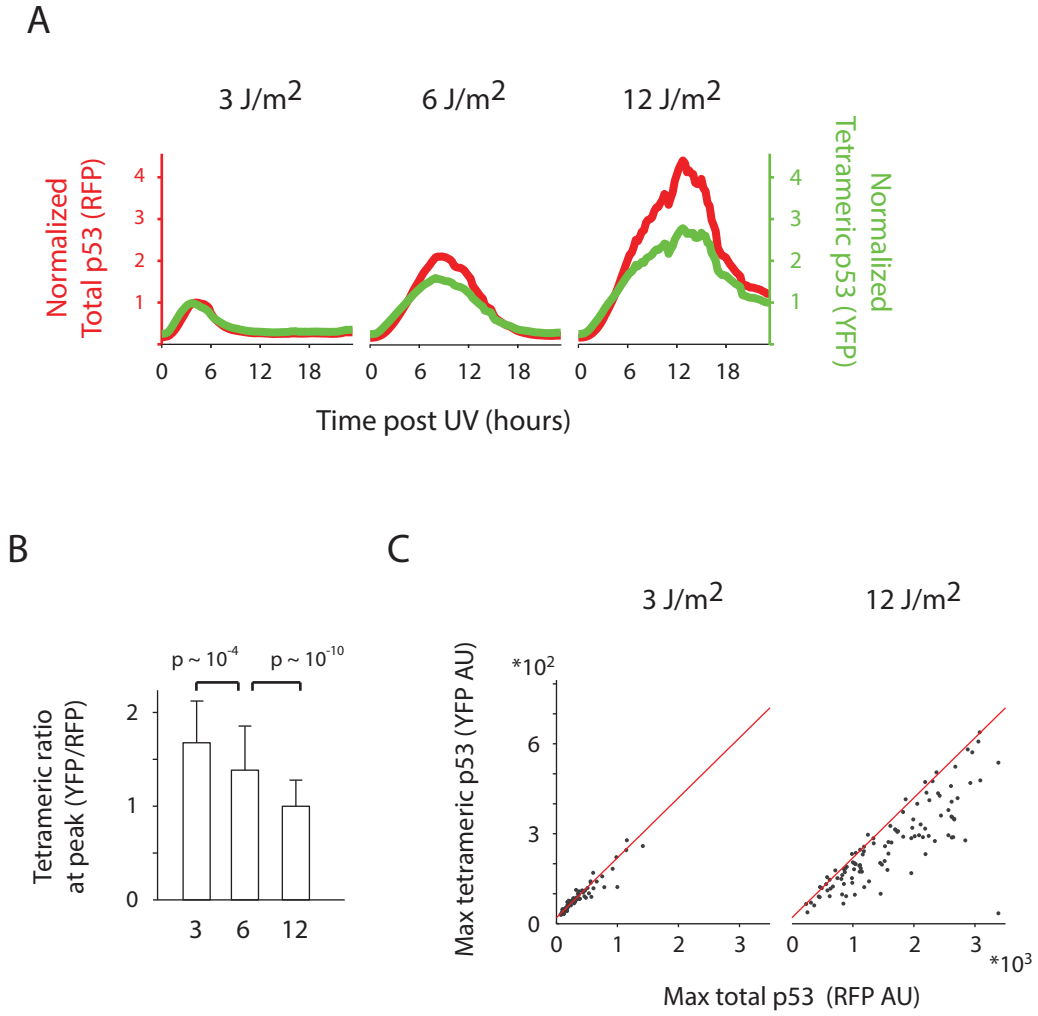

Figure 3.5: Dynamics of total and tetrameric p53 after increasing doses of UV. A. Time traces of the mean fluorescent level under three doses of UV irradiation. Red traces represent total p53 and green represent tetrameric p53 levels. Traces were normalized to the respective maximum level of 3 J/m^2 UV treatment (n = 280). **B.** The ratio of p53 max levels, attained by YFP, over its max tetrameric levels, attained by RFP. Error bars represent standard deviation of the mean. p-values calculated by Mann-Whitney test. **C.** Scatter plot of the RFP peak versus the YFP peak after 3 and 12 J/m^2 UV. Each dot represents one cell. The red line represents the fit obtained from cells following 3 J/m^2, and is presented at 12 J/m^2 as a reference to compare the distributions between damage levels.

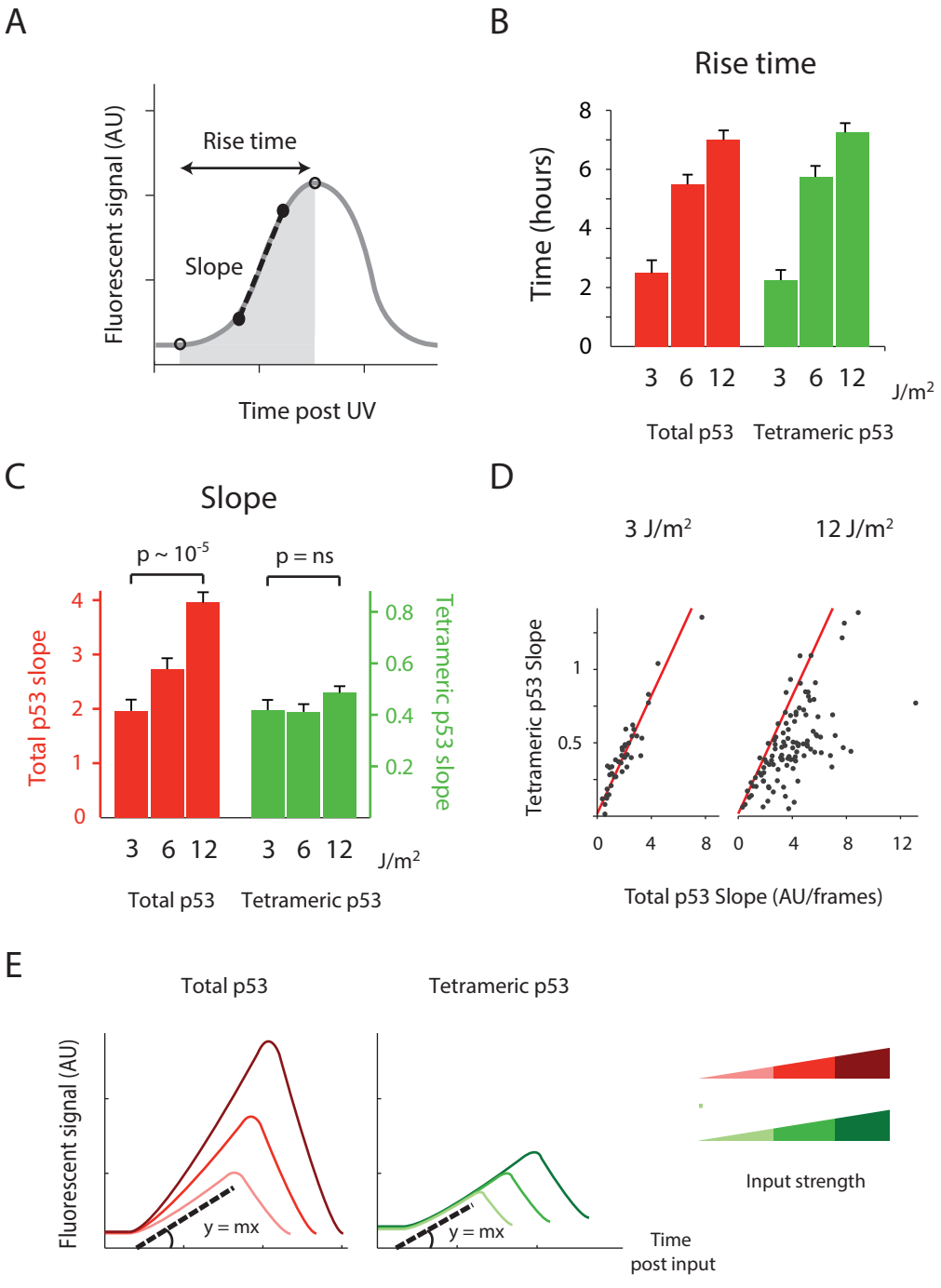
A
Fluorescent signal (AU)
Rise time
Slope
Time post UV
B
Rise time
Time (hours)
8
6
4
2
0
3 6 12 3 6 12
J/m2
Total p53 Tetrameric p53
C
Slope
p ~ 10-5
p = ns
Total p53 slope
Tetrameric p53 slope
4
3
2
1
0
0.8
0.6
0.4
0.2
3 6 12 3 6 12
J/m2
Total p53 Tetrameric p53
D
3 J/m2
12 J/m2
Tetrameric p53 Slope
1
0.5
0 4 8 0 4 8 12
Total p53 Slope (AU/frames)
E
Total p53
Tetrameric p53
Fluorescent signal (AU)
y = mx
y = mx
Input strength
Time
post input

Figure 3.6

Figure 3.6: The rate of p53 tetramers formation is constant across UV doses. A. The dynamics of p53 after UV can be captured by two main parameters: the rise time and the slope of increase. **B-C.** Rise time (B) and slope (C) for total and tetrameric p53 at increasing doses of UV. Shown are median and SEM. n = 210. p-values were calculated by Mann-Whitney test, with p=0.05 as significance threshold. **D.** Scatter plots of the slope of oligomeric versus total p53 after 3 and 12 J/m^2 UV. Each dot represents one cell. The red line represents the fit obtained from cells following 3 J/m^2, and is presented at 12 J/m^2 as a reference to compare the distributions between damage levels. **E.** Schematic drawing recapitulating the data. The rise time increases with input strength for both total and tetrameric p53. The slope "m" increases only for total p53 (red lines) and is constant for tetrameric p53 (green lines).

be explained by a difference in rise time. On the other hand the slope of p53 accumulation showed a different behavior; the slope of total p53 was dose dependent, however the slope of p53 tetramers was constant across all UV doses (Figure 3.6C). This implies that p53 tetramers are formed at a constant rate, regardless of the UV dose. Comparison of the slope at low (3 J/m^2) and high (12 J/m^2) UV doses in individual cells indeed showed that even for cells that accumulate total p53 faster, the rate at which p53 tetramers are formed is fixed and does not follow the rate of total p53 accumulation (Figure 3.6D).

If the dimer-tetramer reaction of p53 were in equilibrium, an increase in the total protein level would result in a proportional increase in the tetrameric level. Instead our results show that the influx of tetramers is fixed across input strength (Figure 3.7). A simple mass-action balance therefore cannot explain our data. The slope conservation of p53 tetramers suggests that there is a regulatory mechanism maintaining a constant rate of tetramer formation independent of the rate at which total p53 accumulates.

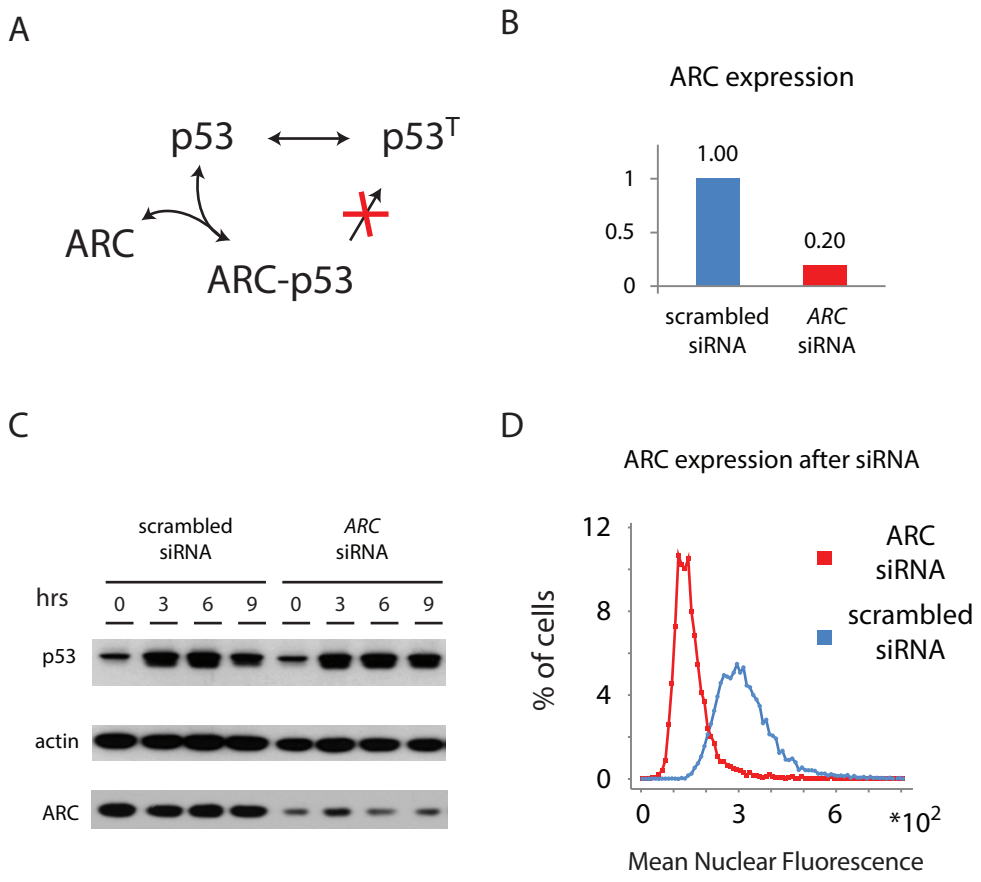

Figure 3.7: ARC knockdown by siRNA. A. The ARC protein binds p53 and interfers with its tetramerization. **B.** qPCR of ARC mRNA under scrambled and ARC siRNA, 48 hrs post trasfection. **C.** Immunoblot of cells following UV at the indicated time points. The levels of ARC are not affected by UV. siRNA against ARC decreases its protein levels. **D.** Distribution of mean nuclear ARC protein measured by immunofluorescence. Knockdown of ARC by siRNA efficiently reduces the amount of ARC protein across cells.

3.2.4 ARC knockdown breaks the slope conservation and leads to enhanced induction of p53 targets

Maintaining a constant rate of tetramer formation could be achieved by sequestering dimers of p53 from becoming tetramers, therefore reducing the pool of tetramers precursor. The apoptosis repressor with caspase recruitment domain (ARC) was previously shown to interact with p53 and disrupt its tetramerization (Figure 3.7A and [67]). To test whether ARC is responsible for the fixed rate at which p53 tetramers are formed, we silenced ARC by siRNA (Figure 3.7B, C and D) and measured the effect on total p53 and p53 tetramers in single cells. The dynamics of total p53 were not affected by ARC knockdown (Figure 3.7B). The maximum level of total p53 in single cells and the slope of total p53 accumulation were not altered in the absence of ARC (Figure 3.8A). Conversely, the dynamics of p53 tetramers were significantly affected by knockdown of ARC; p53 tetramers formed faster as indicated by the increase in both the slope of tetrameric p53 post UV and the higher maximum level (Figure 3.8B). Moreover, silencing ARC disrupted the slope conservation of tetramer formation across UV doses; higher doses of UV led to steeper slope of p53 tetramers formation (Figure 3.8C) and the damping effect was lost (Figure 3.8D).

Does breaking the fixed rate of tetramer formation enhance the transcription of p53 target genes? We measured the induction of p53 target genes after UV treatment with and without ARC. We found that silencing ARC leads to a stronger induction of p53 represented target genes involved in apoptosis and cell cycle arrest (Figure 3.9A) in a p53 dependent manner (Figure 3.9B). This suggests that the increase in the influx of p53 tetramers caused by ARC knockdown boosts p53 activity.

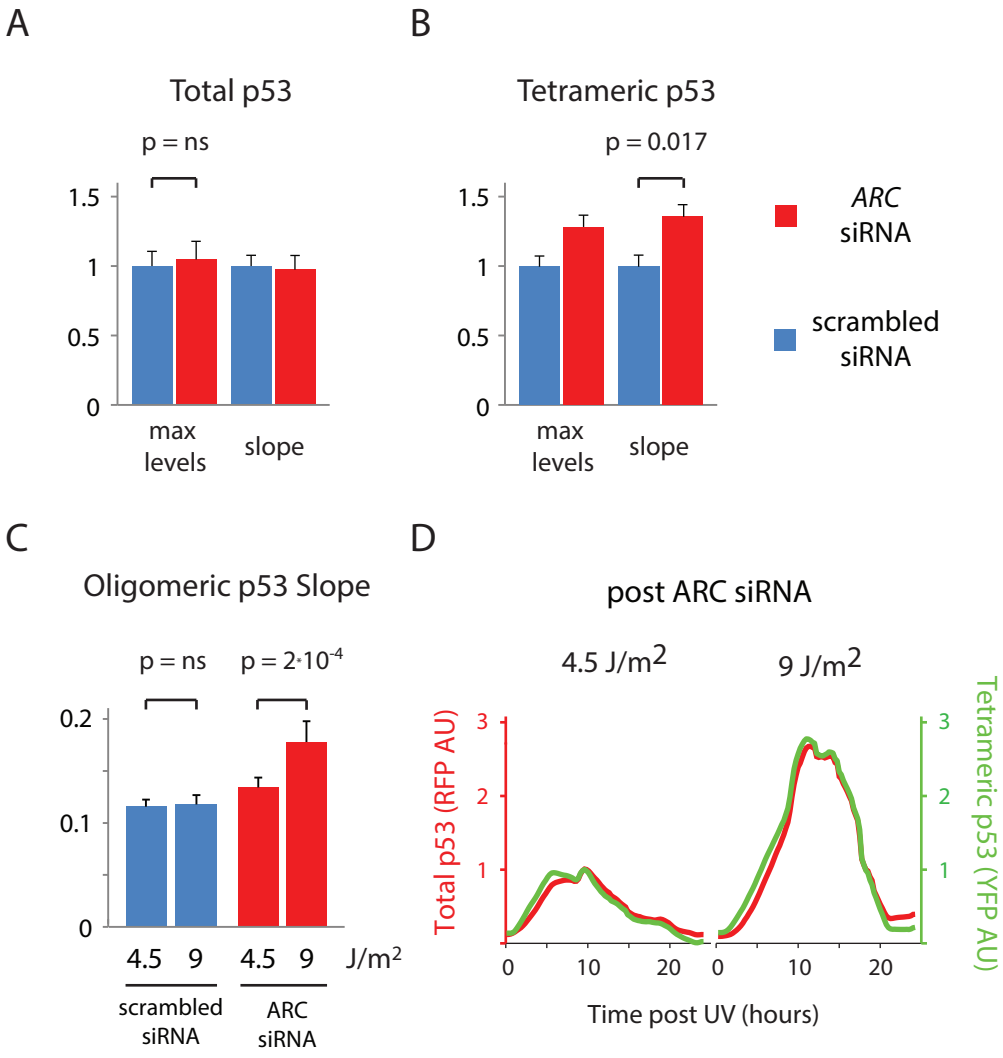

Figure 3.8: ARC knockdown leads to dose-dependent rate of tetramers formation. A. Maximum levels and slope of total p53 after ARC knockdown. **B.** Maximum levels and slope of tetrameric p53 after ARC knockdown. (median and SEM, n=170). ARC knock-down does not affect the maximum and slope of total p53 (p = 0.62) but increases the rate of p53 tetramer accumulation (p = 0.017). **C.** Knockdown of ARC breaks the slope conservation of tetramers formation (median and SEM. n = 360). **D.** Dynamics of total and tetrameric p53 following siRNA against ARC measured by BiFC after UV (time average across cells, traces were normalized to the respective maximum level of 4.5 J/m^2 UV treatment, n = 180). The damping effect on p53 tetramerization is not observed in the absence of ARC.

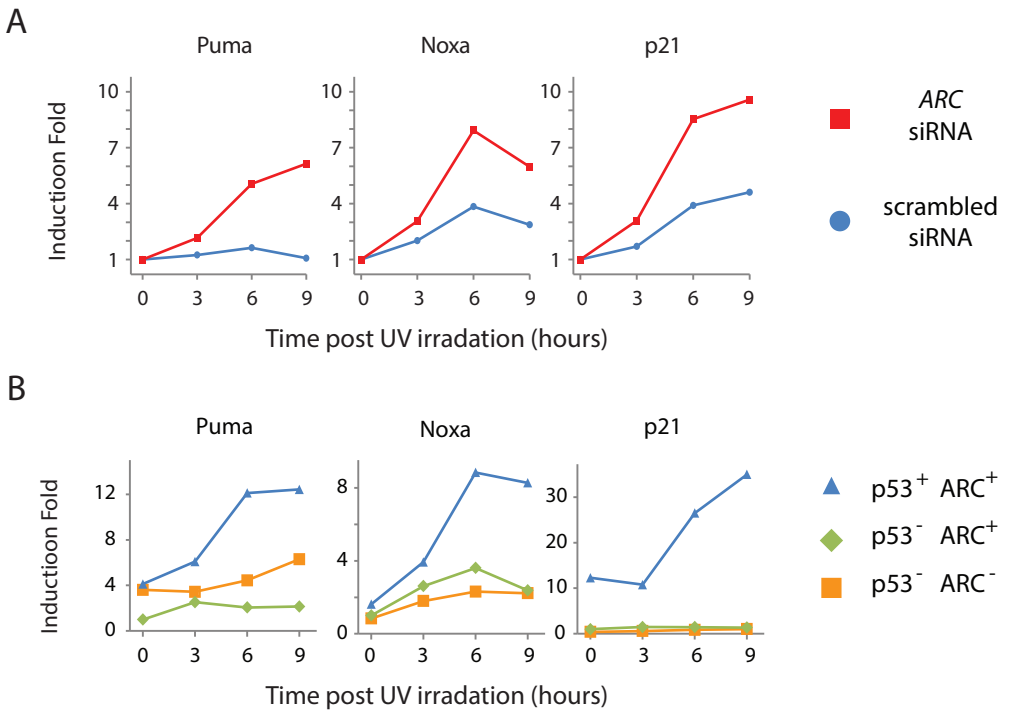

Figure 3.9: ARC knockdown enhances the induction of p53 target expression in a p53-dependent manner. qPCR of p53 target genes mRNA following 6 J/m^2 UV. **A.** Fold induction of p53 targets after ARC siRNA. Knockdown of ARC (red) enhanced the induction of p53 target genes in comparison to scramble siRNA (blue). **B.** The induction of the target genes is contigent on the presence of p53. p53$^-$ indicates cells carrying stable shRNA against p53; ARC$^-$ indicates cells treated with ARC siRNA.

3.3 CONCLUSIONS

Fluorescence protein tagging allows quantification of protein dynamics in live cells and has provided an incredible amount of insight about the anatomy, structure and physiology of the cell [32, 115, 116]. However various features of cellular responses, such as post-translational modifications and oligomerization, are known to affect protein function and are not captured by such fluorescence reporters. In the case of p53, fluorescent tagging enabled quantification of its dynamics in response to various stresses, making important links between specific inputs, p53 dynamics and cell fate [22, 117]. However, the question how well the levels of total p53 represent the levels of functional p53, remains elusive. Here we show that while higher UV doses translate into higher amplitude and longer duration of total p53, the functional units of p53, its tetramers, are formed in a fixed rate regardless of the input strength, leading to a damped response, and potentially buffering against large changes in total p53.

The BiFC method we used in individual cells, together with pull-down assays in populations of cells, confirmed what has previously been suggested in-vitro [55]; that p53 dimerization occurs co-translationally, resulting in homo-dimers in which both monomers are translated from the same mRNA. Many cancers are heterozygotes for p53 and it has been suggested that mutated p53 within a tetramer can abolish the DNA capacity of the entire complex [72, 118]. In agreement, gain of function of p53 due to specific mutations, is not functional when the tetramerization domain is missing [119, 120]. The fact that in cells p53 dimers are homo-dimers indicates that in heterozygous cases the stoichiometry of wild-type and mutant p53 in a tetramer can only be 0:4, 2:2 or 4:0. In the case of a dominant negative mutant this changes the ratio of functional and non-functional complexes, which is im-

portant for our understanding and ability to rescue mutant p53 and enhanced its function in cancer cells.

Constant rate of tetramers formation in face of varying UV doses can theoretically be achieved by two distinct mechanisms: (i) a rate limiting activator of p53 tetramerization, displaying fixed levels and activities independent on the UV dose; (ii) a tunable inhibitor of p53 tetramerization exhibiting stronger inhibition at high levels of UV (Figure 3.1). Such inhibitory strategy allows for total p53 protein to accumulate while the formation of p53 tetramers remains constraint by a tunable valve. In mechanical engineering, such a valve is often used to regulate the flow of a fluid or gas entering an engine, optimizing a desired property of the engine, such as speed, power or fuel efficiency.

Various activators were previously shown to enhance the formation of p53 tetramers, including 14-3-3σ and Hsp70 [57, 121]. While these activators are undoubtedly important for this process, our finding that knock down of ARC allows p53 tetramers to form faster at higher UV doses (Figure 3.9), indicates that the constant rate of tetramers formation in the p53 systems is achieved through inhibition, and not by a rate limiting activator (Figure 3.1). The mechanism by which ARC's competitive inhibition is tuned in response to various UV doses remains an open question. The fact that ARC protein levels do not change after UV suggests that its function requires additional controls such as post-translation modifications or cellular localization [122].

What could be the biological advantages of controlling p53 tetramers with a molecular throttle constraining tetramers formation? p53 triggers crucial outcomes in cells, some are terminal and irreversible. UV, for example leads to cell death. Executing such outcomes at the right time is an important feature of p53 function. A simple linear relationship between UV dose and p53 levels can be dangerous to

cells, as high levels of p53 can activate apoptosis too fast, without allowing cells the time to repair the damage and recover. Fixing the rate at which tetramers are formed disrupts the linear relationship by creating a "brake" in the formation of functional p53, which may be required for protecting cells from prematurely committing to cell death.

A similar idea, yet through a different mechanism, has recently been proposed in the control of DNA damaged induced senescence through p53. Gamma irradiation leads to a series of fixed p53 pulses and to temporary cell cycle arrest [22, 32]. Modulation of p53 dynamics to a sustained non-oscillatory response pushes cells into prematurely committing to senescence. Thus, p53 pulses (in response to gamma) or a fixed rate of tetramer formation (in response to UV) are two examples of cellular mechanisms breaking the linear relationship between input strength and p53 function, presumably protecting cells from committing to irreversible fates.

One of the main goals in cancer therapy is to enhance p53 function in cancer cells. Our ability to understand the various constraints on p53 function through modulation of its dynamics or inhibition of its tetramers has important implications for inducing p53 activity in cells. Specifically, our study suggests that enhancing the efficacy of DNA-damaging drugs can be achieved by combining them with drugs that inhibit ARC, breaking the fixed rate of tetramers formations in cells. Other pathways are known to control cell fate decisions in cells. Developing new tools for measuring their dynamical activity in single cells can help reveal other potential molecular throttles for properly controlling the balance between alternative cellular outcomes.

3.4 Materials and Methods

Cell line construction

The cell line MCF7+p53shRNA was kindly provided by Reuven Agami group [97], Netherlands Cancer Institute, Amsterdam, Netherlands. cDNA for p53 was altered by site-directed mutagenesis (QuikChange kit, Stratagene) at residue 344 to obtain oligomerization mutants p53 L344A and p53 L344P, and with 7 silent point mutations that allow for mRNA to escape shRNA silencing without altering the amino acid sequence. p53 was expressed under the EF1α promoter and tagged with the full red fluorescent protein mKate2 and one of the two fragments of mVenus (mVenus-N, 1-158aa and Venus-C, 159-240aa). The vector was introduced in cells via lentiviral infection and stable clonal selection. Lentiviral particles were produced in 293T cells.

Cell culture and DNA damage

MCF7+p53shRNA+p53-mKate2-mVenus-N/C cells were maintained in RPMI supplemented with 10% fetal calf serum, 100 U/ml penicillin, 100 mg/ml streptomycin, 250 ng/ml fungizone (Gemini Bio-Products) supplemented with selective antibiotics (400 μg/ml G418, 0.5 μg/ml puromycin, 100 μg/mL hygromycin). DNA damage was induced in cells using a UV-C 254nm light source (Ushio). UV was delivered to cells using a UV lamp with a rate of 1.5 J/m^2/s. All UV treatments, therefore, were performed in a single burst lasting < 7s. Cells were harvested for protein/RNA extraction at the indicated times after DNA damage.

Western Blot Analysis

Harvested cells were lysed in the presence of protease and deacetylase inhibitors. Total protein levels were quantified using the BCA assay (Pierce). Equal protein

amounts were separated by electrophoreses on 4%–12% Bis-Tris gradient gels (Invitrogen) and transferred to PVDF membranes by electroblotting. Membranes were blocked with 5% nonfat dried milk, incubated overnight with primary antibody, washed, incubated with secondary antibody coupled to peroxidase. Protein levels were detected with chemoluminiscence (ECL plus, Amersham). p53 dynamics were quantified by normalizing total p53 levels (DO1, Santa Cruz) to alpha-actin (Sigma). ARC was detected with a polyclonal antobody against ARC (Cayman Chemical, 160737).

Target gene expression dynamics

Total RNA was extracted using the RNeasy protocol (Qiagen). RNA concentration was determined by measuring absorbance at 260 nm. Equal RNA levels were used to generate complementary DNA using the high-capacity cDNA reverse transcription protocol (Applied Biosystems). Quantitative PCR was performed using reaction mixtures of 8.4 ng total RNA, 100 nM primer, and SYBR Green reagent (Applied Biosystems).

Time-lapse Microscopy

Two days before microscopy, cells were grown on poly-D-lysinecoated glass-bottom plates (MatTek Corporation) in transparent medium supplemented with 5% fetal calf serum, 100 U/ml penicillin, 100 μg/ml streptomycin, and 250 ng/ml fungizone (Gemini Bio-Products). Cells were imaged with a Nikon Eclipse Ti-inverted fluorescence microscope on which the stage was surrounded by an enclosure to maintain constant temperature, CO_2 concentration, and humidity. Images were acquired every 15 min. The mVenus filter set was 500/20x excitation, 515nm dichroic beam splitter, and 535/30m emission (Chroma). The mKate2 filter set was 560/40x excitation, 585nm dichroic beam splitter, and 630/75m emission (Chroma). We an-

alyzed images using MetaMorph software (Molecular Devices) and custom written MATLAB software (Mathworks), which is available upon request.

RNAi

To knockdown ARC we used siGENOME SMARTpool of siRNA against the NOL3 gene mRNA (Dharmacon). For all controls we used the scrambled siRNA from QUIAGEN (AllStars Negative Control siRNA, Qiagen 1027280). We performed all RNA transfection using DharmaFECT 1 transfection reagent following the manufacturer's protocol (Dharmacon). We assayed the knockdown of NOL3 48 hr after transfection.

Co-Immunoprecipitation assay

MCF7 p53shRNA cells were infected with lentivirus expressing pEF1a-p53wt-CFP and pEF1a-p53(wt/L344A/L344P)-HA and selected by antibiotic resistance. Cells were treated with 400 ng/μl neocarzinostatin (NCS, Sigma) and collected after 2.5 hrs. Cell lysate were obtained with lysis buffer without SDS (TNTE /1% Triton buffer supplemented with protease and phosphatase inhibitors) passing samples through 20G needle 10X at 4°C then spun down in chilled table top centrifuge for 30min. Lysates were incubated for 1 hour at 4°C in rotating shaker with monoclonal anti-HA-agarose beads (A2095, Sigma) pre-washed 3X in TNTE buffer. Lysate-beads solutions were washed 3X in TNTE buffer then resuspended in 4X LDS buffer and boiled at 95°C for 3 min.

Immunofluorescence

Cells were grown on coverslips coated with poly-L-lysine and fixed with 2% paraformaldehyde for 15 min at RT. Cells were permeabilized with 5 min incubation in 100% methanol at -20°C, washed in PBS, incubated with primary antibody against ARC

(Cayman Chemical, 160737), washed, and incubated with secondary antibody coupled to Alexa555. After washing, cells were stained with DAPI and embedded in Prolong Antifade (Invitrogen). Images were acquired with a 20x plan apo objective (NA 0.75) with the CY3 filter set (sp102v1, Chroma). Automated segmentation was performed in Matlab (MathWorks). 5,000-8,000 cells were measured per condition.

3.5 Author Contributions

Giorgio Gaglia and Galit Lahav designed the research. Giorgio Gaglia conducted the experiments and performed the analysis. Giorgio Gaglia and Galit Lahav wrote the paper.

Chapter 4: Discussion

4.1 Reactivating p53 in cells

Through this work I aimed to investigate the control of p53 homo-tetramerization and to demonstrate that inducing tetramerization can trigger activation of p53 function. I used two types of DNA damage that are known to activate p53 and have been instrumental to demonstrate the correlation between tetramerization and transcriptional activity. This was possible as I have been able to precisely quantify the amount of tetramerized p53. Moreover I started elucidating the co-factors that regulate p53 tetramerization in cells and what their role is.

The high rate of mutations in the p53 pathway observed in cancers underscores its importance in preventing uncontrolled proliferation. The most common alterations in p53 lead to loss of its function as a transcription factor. Hence the strategies that have been used to target p53 defective tumors are centered in attempting to restore functionality. One promising approach involves increasing p53 protein concentration by targeting its interaction with Mdm2. Such approaches led to the development of drugs like Nutlin [123] and RITA [124]. Another approach im-

plicates reactivating the function mutant p53 with drugs that bind the protein core [125]. Another possibility that emerged from my studies is to push the existing pool of p53 into its tetrameric conformation, and by this boosting its activity. However the in vivo understanding of the control and function of tetramerization is limited. The aim of this work was to develop methods for studying homo-oligomerization in live cells and to advance the understanding of the p53 tetramerization reaction.

4.2 Advancements in quantification of homo-oligomerization in live single cells

I developed and applied two complementary methods in this study, fluorescence correlation spectroscopy (FCS) and bimolecular fluorescence complementation (BiFC). Both methods enable measuring total p53 protein and p53 tetramerization simultaneously, dynamically and in living single cells; all features that are fundamental to study p53 tetramerization. While the mechanics of the oligomerization reaction in isolation have been worked out in detail *in vitro*, in living cells co-factors and post-translational modification affect p53 regulation. Moreover, after cellular stress the levels of p53 protein undergo complex dynamics that can drive the oligomerization reaction and confound the understanding of its regulation. Hence monitoring the tetramerization state together with its protein level is essential.

The difference between the FCS and the BiFC measurements consists in the trade-off between precision and time resolution. The oligomeric state of p53 spans a small dynamic range between dimerization and tetramerization. FCS provides adequately precise quantification of the aggregation state to calculate the distribution of p53 oligomers prior to perturbation, and dissect the molecular events triggered by DNA damage at resolution of less than one hour. However FCS has a low throughput, allowing the measurement of fewer than 10 cells in the same ex-

periment for only up to a few hours. In contrast BiFC is based on epifluorescence microscopy, which allows the tracking of tens of cells simultaneously in a set of diverse conditions. The maturation of the reassembled fluorescent proteins does not allow for a short time resolution but the experimental setup enables following cells for multiple days. The complementarity of these methods allowed us to study the behavior of p53 tetramers after DNA damage caused by two sources, radiomimetic drugs and ultraviolet radiation, which have been shown to cause different temporal dynamics of p53 protein levels.

4.3 Rapid activation of p53 oligomerization after DNA damage

After double strand breaks (generated by IR or IR-mimicking agents) p53 shows a digital response with pulses of protein accumulation roughly 5 hours long and with conserved amplitude and frequency [32]. At the end of each pulse, recurrent activation of the pathway leads to either another full pulse or no induction at all [35]. Moreover increasing doses of damage lead to more pulses rather than modifying the pulse characteristics. Even though it is unclear whether the induction of each pulse is molecularly identical, these observations suggest that the key activation events occur in the first couple of hours after damage. Using FCS I measured p53 tetramerization during the induction of the first pulse and I showed how the formation of p53 tetramers occurs before the accumulation of p53 protein and even in its absence. Given the higher rate of tetramers degradation, the parallel induction of tetramerization and total protein suggests the presence of specific regulation to induce the accumulation of tetramers. Importantly I decoupled the increase of p53 oligomers from the protein abundance and showed that the transcriptional function of p53 is also increased just by p53 oligomerization.

The mechanism of upregulation of p53 tetramerization after double strand breaks is not known. Tetramerization occurs rapidly and this strongly suggests that the regulation is not transcriptional but rather based on co-factor binding and post-translational modifications. *In vitro* studies have shown that certain modifications can stabilize the p53 tetramers. For instance phosphorylations at residues Ser366, Ser378 and Thr387 lead to binding of p53 to 14-3-3 proteins, decreasing the tetrameric dissociation constant by up to 10-fold [57]. Furthermore, phosphorylation at Ser392 and dephosphorylation of Ser315 directly increase p53 self-affinity [58]. Other modifications are known to require tetramerization in order to happen, such as phosphorylation at Ser20 and C-terminal lysines acetylation [75, 126]. Applying FCS to mutants constitutively modified, for example by phospho-mimic amino acid substitutions, would be insightful to understand to what extent these modifications affect p53 tetramerization in cells.

The applications of the FCS measurements are potentially extremely broad. Firstly they allow to measure oligomerization in different cell compartments, thanks to the small volume of observation relative the size of a human cell. For instance p53 is known to relocate to the mitochondria and to induce apoptosis by inhibiting anti-apoptotic proteins such as Bcl2 and BclX. Hence an interesting question that could be answered with our experimental setup is whether p53 does so as a dimer or as a tetramer. More generally this method could be used to measure aggregation of virtually any protein in the cell. The only limitation is posed by the cellular concentration of the protein; this needs to be low enough for the diffusion of the molecules to and from the observation volume to produce significant fluctuations in the fluorescent intensity signal.

4.4 A MOLECULAR MECHANISM KEEPING THE RATE OF P53 TETRAMERIZATION CONSTANT

In contrast to the digital response to double strand break, UV induced DNA damage triggers a single pulse of p53 accumulation, the height and the duration of which are UV dose-dependent. The lengthen time scale and the need for varying doses of UV damage made the BiFC method more suitable to study tetramerization of p53 in this context.

First I demonstrated how dimerization of p53 is co-translational in cells, confirming a feature that was previously postulated from an *in vitro* translation experiment [55]. More precisely I showed that proteins expressed from different alleles of p53 do not mix at the dimer level, during or after translation. This is in agreement with the strong dimeric binding constant measured *in vitro*, but it is in contrast with other evidence showing that co-factors of p53, such as members of the S100 protein family, are able to induce monomerization of p53 dimers in the test tube [99]. The latter occurrence is not likely in our experiment as I performed them in MCF7 cells that do not express these members of the S100 family. In FCS I observed a population of free p53 monomers, but I did not observe subunit exchange between dimers. These observations suggest that once the chance to dimerize near the ribosome is missed, then the p53 monomers remain monomeric and do not form dimers. On top of this, the rate of dimerization likely increases after DNA damage, since the fraction of monomers decreases in time. The yet unknown mechanism that controls co-translationality of dimerization has important implications for mutant p53, because it implies that mutations of p53 affect both proteins in every dimer. Hence in p53 heterozygous cells the interaction between wild-type and mutated p53, which is the basis of the dominant negative effect, occurs only at the tetrameric interface

level.

I also showed that, while the tetramerization reaction after double strand breaks is activated, increasing doses of UV actually dampened the binding between p53 dimers. Despite the fact that the rate of total p53 increases in parallel with the increase of radiation, the system features a constant rate of tetramer formation. I envision this mechanism as a tunable molecular valve, or a throttle, which constrains the entry into the tetrameric state making it steady in spite of a varying amount of available total p53. Since p53 transcriptional activity requires tetramerization, the throttle steadies the transcription of target genes. However it is not intuitive why such a constraint would be beneficial, especially since increased damage does create more stress to the cell. One possibility is that the constant rate of tetramerization makes p53 tetramer levels work as a timer. The steady increase of tetramers stands for the signal being "on" and the length of the pulse, which is still dose-dependent, reports for the time at which the signal is turned "off". Another possibility is that the pool of p53 dimers plays a functional role, probably not transcriptional, and that the system is actually increasing the dimer population to enhance a specific function, yet to be unveiled.

I observed that at increasing the doses of UV radiation the tetrameric fraction is reduced. This suggested a negative regulation on tetramerization and I confirmed this hypothesis by identifying ARC, i.e. apoptotic repressor with CARD domain as part of the inhibitory process. While ARC is a necessary part of the molecular throttle, it is unlikely that it works alone, especially since ARC's protein level does not increase after DNA damage. Either other proteins form a complex with ARC to inhibit tetramerization or ARC's activity is dependent on post-translational modifications that are altered after damage. By knocking-down ARC I showed that downregulation of the throttle leads to an increase in p53 transcriptional activity.

Moreover since ARC knockdown did not affect the p53 protein levels, this is attributable specifically to the increase in tetramerization.

4.5 Future directions

The work in this thesis highlighted novel instances of regulation of p53 function through modulation of tetramerization. It showed that, irrespective of the levels of p53 protein, additional factors influence tetramerization, either inducing or inhibiting it. These findings open two avenues of research: to investigate the molecular basis of these regulatory processes and to chemically alter the tetrameric balance for possible therapeutic applications. In both cases the BiFC system described in Chapter 3 can be employed to perform a screen to identify putative candidates, while the FCS setup from Chapter 2 would be used to validate the screen's hits.

The siRNA approach used to assay for ARC's inhibition of tetramerization in Chapter 3, can be extended into a genetic screen with pooled barcoded shRNA's. Two-color FACS would be used to isolate the population of cells with highest tetrameric p53 levels, relative to the total p53 amount, which would then be analyzed by next-generation sequencing to recover the potential hits. This assay would unbiasedly probe for other negative regulators of p53 tetramerization. However, since there are a number of putative p53 cofactors already known, a global search could also be combined or substituted with custom shRNA libraries specifically targeting these cofactors [127, 128].

Another interesting direction is to use an imaging-based approach to screen for compounds that either upregulate or downregulate tetramerization. In cancer models with wild-type p53 the aim of the screen would be to identify drugs that boost tetramerization, in the hope of enhancing p53 activity. On the other hand, compounds that inhibit tetramerization would also be extremely useful, for instance

in the case of cells heterozygous for p53. Here the product of a DNA-binding defective allele is thought to oligomerize with wild-type p53, interfering with the latter's activity, in the so-called dominant negative effect. The BiFC experimental system can be readily modified to combine expression of a wild-type copy of p53 together with a mutant counterpart; the complementation assay would then report for hetero-oligomerization of p53 mutant and wild-type. With this setup, a chemical screen could then be applied to identify compounds that specifically disrupt the mutant to wild-type interaction, rescuing the function the wild-type.

In conclusion, the work in this thesis shows that the ability to reliably measure p53 tetramerization has been instrumental to demonstrating directly the relationship between tetramerization and transcriptonal activity of p53. Moreover, p53 is only one example of how homo-oligomerization is used to control function. The methods developed and discussed in this work can be applied to many other proteins in the cell. The methods' complementarity allows for spatial resolution of cellular compartments and both short and long timescales, making them widely applicable to ask fundamental and novel questions about the dynamics of protein homo-oligomerization in live single cells.

Bibliography

[1] F. Murray-Zmijewski, E. A. Slee, and X. Lu, "A complex barcode underlies the heterogeneous response of p53 to stress," *Nat Rev Mol Cell Biol*, vol. 9, no. 9, pp. 702–12, 2008.

[2] A. Vilborg, M. T. Wilhelm, and K. G. Wiman, "Regulation of tumor suppressor p53 at the rna level," *J Mol Med (Berl)*, vol. 88, no. 7, pp. 645–52, 2010.

[3] N. D. Lakin and S. P. Jackson, "Regulation of p53 in response to dna damage," *Oncogene*, vol. 18, no. 53, pp. 7644–55, 1999.

[4] M. B. Kastan, O. Onyekwere, D. Sidransky, B. Vogelstein, and R. W. Craig, "Participation of p53 protein in the cellular response to dna damage," *Cancer Res*, vol. 51, no. 23 Pt 1, pp. 6304–11, 1991.

[5] D. R. Green and G. Kroemer, "Cytoplasmic functions of the tumour suppressor p53," *Nature*, vol. 458, no. 7242, pp. 1127–30, 2009.

[6] J. E. Chipuk, L. Bouchier-Hayes, T. Kuwana, D. D. Newmeyer, and D. R. Green, "Puma couples the nuclear and cytoplasmic proapoptotic function of p53," *Science*, vol. 309, no. 5741, pp. 1732–5, 2005.

[7] E. Tasdemir, M. C. Maiuri, L. Galluzzi, I. Vitale, M. Djavaheri-Mergny, M. D'Amelio, A. Criollo, E. Morselli, C. Zhu, F. Harper, U. Nannmark, C. Samara, P. Pinton, J. M. Vicencio, R. Carnuccio, U. M. Moll, F. Madeo, P. Paterlini-Brechot, R. Rizzuto, G. Szabadkai, G. Pierron, K. Blomgren, N. Tavernarakis, P. Codogno, F. Cecconi, and G. Kroemer, "Regulation of autophagy by cytoplasmic p53," *Nat Cell Biol*, vol. 10, no. 6, pp. 676–87, 2008.

[8] T. Riley, E. Sontag, P. Chen, and A. Levine, "Transcriptional control of human p53-regulated genes," *Nat Rev Mol Cell Biol*, vol. 9, no. 5, pp. 402–12, 2008.

[9] A. M. Bode and Z. Dong, "Post-translational modification of p53 in tumorigenesis," *Nat Rev Cancer*, vol. 4, no. 10, pp. 793–805, 2004.

[10] R. Honda, H. Tanaka, and H. Yasuda, "Oncoprotein mdm2 is a ubiquitin ligase e3 for tumor suppressor p53," *FEBS Lett*, vol. 420, no. 1, pp. 25–7, 1997.

[11] F. Toledo and G. M. Wahl, "Regulating the p53 pathway: in vitro hypotheses, in vivo veritas," *Nat Rev Cancer*, vol. 6, no. 12, pp. 909–23, 2006.

[12] S. N. Jones, A. E. Roe, L. A. Donehower, and A. Bradley, "Rescue of embryonic lethality in mdm2-deficient mice by absence of p53," *Nature*, vol. 378, no. 6553, pp. 206–8, 1995.

[13] M. A. Lohrum, D. B. Woods, R. L. Ludwig, E. Balint, and K. H. Vousden, "C-terminal ubiquitination of p53 contributes to nuclear export," *Mol Cell Biol*, vol. 21, no. 24, pp. 8521–32, 2001.

[14] T. Buschmann, V. Adler, E. Matusevich, S. Y. Fuchs, and Z. Ronai, "p53 phosphorylation and association with murine double minute 2, c-jun nh2-terminal kinase, p14arf, and p300/cbp during the cell cycle and after exposure to ultraviolet irradiation," *Cancer Res*, vol. 60, no. 4, pp. 896–900, Feb 2000.

[15] S. L. Harris and A. J. Levine, "The p53 pathway: positive and negative feedback loops," *Oncogene*, vol. 24, no. 17, pp. 2899–908, 2005.

[16] Y. Barak, T. Juven, R. Haffner, and M. Oren, "mdm2 expression is induced by wild type p53 activity," *EMBO J*, vol. 12, no. 2, pp. 461–8, 1993.

[17] R. P. Leng, Y. Lin, W. Ma, H. Wu, B. Lemmers, S. Chung, J. M. Parant, G. Lozano, R. Hakem, and S. Benchimol, "Pirh2, a p53-induced ubiquitin-protein ligase, promotes p53 degradation," *Cell*, vol. 112, no. 6, pp. 779–91, 2003.

[18] D. Dornan, I. Wertz, H. Shimizu, D. Arnott, G. D. Frantz, P. Dowd, K. O'Rourke, H. Koeppen, and V. M. Dixit, "The ubiquitin ligase cop1 is a critical negative regulator of p53," *Nature*, vol. 429, no. 6987, pp. 86–92, 2004.

[19] R. B. Setlow, P. A. Swenson, and W. L. Carrier, "Thymine dimers and inhibition of dna synthesis by ultraviolet irradiation of cells," *Science*, vol. 142, no. 3598, pp. 1464–6, 1963.

[20] S. de Feraudy, K. Ridd, L. M. Richards, P. Y. Kwok, I. Revet, D. Oh, L. Feeney, and J. E. Cleaver, "The dna damage-binding protein xpc is a frequent target for inactivation in squamous cell carcinomas," *Am J Pathol*, vol. 177, no. 2, pp. 555–62, 2010.

[21] J. E. Cleaver, "Cancer in xeroderma pigmentosum and related disorders of dna repair," *Nat Rev Cancer*, vol. 5, no. 7, pp. 564–73, 2005.

[22] J. E. Purvis, K. W. Karhohs, C. Mock, E. Batchelor, A. Loewer, and G. Lahav, "p53 dynamics control cell fate," *Science*, vol. 336, no. 6087, pp. 1440–4, 2012.

[23] X. Zeng, D. Keller, L. Wu, and H. Lu, "Uv but not gamma irradiation accelerates p53-induced apoptosis of teratocarcinoma cells by repressing mdm2 transcription," *Cancer Res*, vol. 60, no. 21, pp. 6184–8, 2000.

[24] D. V. Bulavin, S. Saito, M. C. Hollander, K. Sakaguchi, C. W. Anderson, E. Appella, and J. Fornace, A. J., "Phosphorylation of human p53 by p38 kinase coordinates n-terminal phosphorylation and apoptosis in response to uv radiation," *EMBO J*, vol. 18, no. 23, pp. 6845–54, 1999.

[25] A. Bar-Shira, S. Rashi-Elkeles, L. Zlochover, L. Moyal, N. I. Smorodinsky, R. Seger, and Y. Shiloh, "Atm-dependent activation of the gene encoding map kinase phosphatase 5 by radiomimetic dna damage," *Oncogene*, vol. 21, no. 5, pp. 849–55, 2002.

[26] I. H. Goldberg, "Mechanism of neocarzinostatin action: role of dna microstructure in determination of chemistry of bistranded oxidative damage." *Accounts of chemical research*, vol. 24, no. 7, pp. 191–198, 1991.

[27] R. S. Tibbetts, K. M. Brumbaugh, J. M. Williams, J. N. Sarkaria, W. A. Cliby, S. Y. Shieh, Y. Taya, C. Prives, and R. T. Abraham, "A role for atr in the dna damage-induced phosphorylation of p53," *Genes Dev*, vol. 13, no. 2, pp. 152–7, 1999.

[28] Q. Liu, S. Guntuku, X. S. Cui, S. Matsuoka, D. Cortez, K. Tamai, G. Luo, S. Carattini-Rivera, F. DeMayo, A. Bradley, L. A. Donehower, and S. J. Elledge, "Chk1 is an essential kinase that is regulated by atr and required for the g(2)/m dna damage checkpoint," *Genes Dev*, vol. 14, no. 12, pp. 1448–59, 2000.

[29] A. Hirao, Y. Y. Kong, S. Matsuoka, A. Wakeham, J. Ruland, H. Yoshida, D. Liu, S. J. Elledge, and T. W. Mak, "Dna damage-induced activation of p53 by the checkpoint kinase chk2," *Science*, vol. 287, no. 5459, pp. 1824–7, 2000.

[30] C. J. Bakkenist and M. B. Kastan, "Dna damage activates atm through intermolecular autophosphorylation and dimer dissociation," *Nature*, vol. 421, no. 6922, pp. 499–506, 2003.

[31] M. F. Lavin and N. Gueven, "The complexity of p53 stabilization and activation," *Cell Death Differ*, vol. 13, no. 6, pp. 941–50, 2006.

[32] G. Lahav, N. Rosenfeld, A. Sigal, N. Geva-Zatorsky, A. J. Levine, M. B. Elowitz, and U. Alon, "Dynamics of the p53-mdm2 feedback loop in individual cells," *Nat Genet*, vol. 36, no. 2, pp. 147–50, 2004.

[33] E. Batchelor, A. Loewer, C. Mock, and G. Lahav, "Stimulus-dependent dynamics of p53 in single cells," *Mol Syst Biol*, vol. 7, p. 488, 2011.

[34] R. Lev Bar-Or, R. Maya, L. A. Segel, U. Alon, A. J. Levine, and M. Oren, "Generation of oscillations by the p53-mdm2 feedback loop: a theoretical and experimental study," *Proc Natl Acad Sci U S A*, vol. 97, no. 21, pp. 11 250–5, Oct 2000.

[35] E. Batchelor, C. S. Mock, I. Bhan, A. Loewer, and G. Lahav, "Recurrent initiation: a mechanism for triggering p53 pulses in response to dna damage," *Mol Cell*, vol. 30, no. 3, pp. 277–89, 2008.

[36] A. Loewer, E. Batchelor, G. Gaglia, and G. Lahav, "Basal dynamics of p53 reveal transcriptionally attenuated pulses in cycling cells," *Cell*, vol. 142, no. 1, pp. 89–100, 2010.

[37] L. A. Carvajal and J. J. Manfredi, "Another fork in the road–life or death decisions by the tumour suppressor p53," *EMBO Rep*, vol. 14, no. 5, pp. 414–21, 2013.

[38] K. Hashimoto and A. R. Panchenko, "Mechanisms of protein oligomerization, the critical role of insertions and deletions in maintaining different oligomeric states," *Proc Natl Acad Sci U S A*, vol. 107, no. 47, pp. 20 352–7, 2010.

[39] N. J. Marianayagam, M. Sunde, and J. M. Matthews, "The power of two: protein dimerization in biology," *Trends Biochem Sci*, vol. 29, no. 11, pp. 618–25, 2004.

[40] M. H. Ali and B. Imperiali, "Protein oligomerization: how and why," *Bioorg Med Chem*, vol. 13, no. 17, pp. 5013–20, 2005.

[41] F. Wade, A. Espagne, M. A. Persuy, J. Vidic, R. Monnerie, F. Merola, E. Pajot-Augy, and G. Sanz, "Relationship between homo-oligomerization of a mammalian olfactory receptor and its activation state demonstrated by bioluminescence resonance energy transfer," *J Biol Chem*, vol. 286, no. 17, pp. 15 252–9, 2011.

[42] T. Hattori, N. Ohoka, Y. Inoue, H. Hayashi, and K. Onozaki, "C/ebp family transcription factors are degraded by the proteasome but stabilized by forming dimer," *Oncogene*, vol. 22, no. 9, pp. 1273–80, 2003.

[43] B. Antonsson, S. Montessuit, S. Lauper, R. Eskes, and J. C. Martinou, "Bax oligomerization is required for channel-forming activity in liposomes and to trigger cytochrome c release from mitochondria," *Biochem J*, vol. 345 Pt 2, pp. 271–8, 2000.

[44] A. C. Joerger and A. R. Fersht, "Structural biology of the tumor suppressor p53," *Annu Rev Biochem*, vol. 77, pp. 557–82, 2008.

[45] P. D. Jeffrey, S. Gorina, and N. P. Pavletich, "Crystal structure of the tetramerization domain of the p53 tumor suppressor at 1.7 angstroms," *Science*, vol. 267, no. 5203, pp. 1498–502, 1995.

[46] D. B. Veprintsev, S. M. Freund, A. Andreeva, S. E. Rutledge, H. Tidow, J. M. Canadillas, C. M. Blair, and A. R. Fersht, "Core domain interactions in full-length p53 in solution," *Proc Natl Acad Sci U S A*, vol. 103, no. 7, pp. 2115–9, 2006.

[47] M. G. Mateu and A. R. Fersht, "Nine hydrophobic side chains are key determinants of the thermodynamic stability and oligomerization status of tumour suppressor p53 tetramerization domain," *EMBO J*, vol. 17, no. 10, pp. 2748–58, May 1998.

[48] M. Kitayner, H. Rozenberg, N. Kessler, D. Rabinovich, L. Shaulov, T. E. Haran, and Z. Shakked, "Structural basis of dna recognition by p53 tetramers," *Mol Cell*, vol. 22, no. 6, pp. 741–53, 2006.

[49] M. Wells, H. Tidow, T. J. Rutherford, P. Markwick, M. R. Jensen, E. Mylonas, D. I. Svergun, M. Blackledge, and A. R. Fersht, "Structure of tumor suppressor p53 and its intrinsically disordered n-terminal transactivation domain," *Proc Natl Acad Sci U S A*, vol. 105, no. 15, pp. 5762–7, 2008.

[50] H. Tidow, R. Melero, E. Mylonas, S. M. Freund, J. G. Grossmann, J. M. Carazo, D. I. Svergun, M. Valle, and A. R. Fersht, "Quaternary structures of tumor suppressor p53 and a specific p53 dna complex," *Proc Natl Acad Sci U S A*, vol. 104, no. 30, pp. 12 324–9, 2007.

[51] P. V. Nikolova, J. Henckel, D. P. Lane, and A. R. Fersht, "Semirational design of active tumor suppressor p53 dna binding domain with enhanced stability," *Proc Natl Acad Sci U S A*, vol. 95, no. 25, pp. 14 675–80, 1998.

[52] K. H. Khoo, A. Andreeva, and A. R. Fersht, "Adaptive evolution of p53 thermodynamic stability," *J Mol Biol*, vol. 393, no. 1, pp. 161–75, 2009.

[53] S. Rajagopalan, F. Huang, and A. R. Fersht, "Single-molecule characterization of oligomerization kinetics and equilibria of the tumor suppressor p53," *Nucleic Acids Res*, vol. 39, no. 6, pp. 2294–303, 2011.

[54] M. G. Mateu, M. M. Sanchez Del Pino, and A. R. Fersht, "Mechanism of folding and assembly of a small tetrameric protein domain from tumor suppressor p53," *Nat Struct Biol*, vol. 6, no. 2, pp. 191–8, 1999.

[55] C. D. Nicholls, K. G. McLure, M. A. Shields, and P. W. Lee, "Biogenesis of p53 involves cotranslational dimerization of monomers and posttranslational dimerization of dimers. implications on the dominant negative effect," *J Biol Chem*, vol. 277, no. 15, pp. 12 937–45, 2002.

[56] R. L. Weinberg, D. B. Veprintsev, and A. R. Fersht, "Cooperative binding of tetrameric p53 to dna," *J Mol Biol*, vol. 341, no. 5, pp. 1145–59, 2004.

[57] S. Rajagopalan, A. M. Jaulent, M. Wells, D. B. Veprintsev, and A. R. Fersht, "14-3-3 activation of dna binding of p53 by enhancing its association into tetramers," *Nucleic Acids Res*, vol. 36, no. 18, pp. 5983–91, 2008.

[58] K. Sakaguchi, H. Sakamoto, M. S. Lewis, C. W. Anderson, J. W. Erickson, E. Appella, and D. Xie, "Phosphorylation of serine 392 stabilizes the tetramer formation of tumor suppressor protein p53," *Biochemistry*, vol. 36, no. 33, pp. 10 117–24, 1997.

[59] L. Ma, J. Wagner, J. J. Rice, W. Hu, A. J. Levine, and G. A. Stolovitzky, "A plausible model for the digital response of p53 to dna damage," *Proc Natl Acad Sci U S A*, vol. 102, no. 40, pp. 14 266–71, 2005.

[60] K. G. McLure and P. W. Lee, "How p53 binds dna as a tetramer," *EMBO J*, vol. 17, no. 12, pp. 3342–50, 1998.

[61] V. A. Yakovlev, A. S. Bayden, P. R. Graves, G. E. Kellogg, and R. B. Mikkelsen, "Nitration of the tumor suppressor protein p53 at tyrosine 327 promotes p53 oligomerization and activation," *Biochemistry*, vol. 49, no. 25, pp. 5331–9, 2010.

[62] Y. Kawaguchi, A. Ito, E. Appella, and T. P. Yao, "Charge modification at multiple c-terminal lysine residues regulates p53 oligomerization and its nucleus-cytoplasm trafficking," *J Biol Chem*, vol. 281, no. 3, pp. 1394–400, 2006.

[63] H. Y. Yang, Y. Y. Wen, C. H. Chen, G. Lozano, and M. H. Lee, "14-3-3 sigma positively regulates p53 and suppresses tumor growth," *Mol Cell Biol*, vol. 23, no. 20, pp. 7096–107, 2003.

[64] S. Hanson, E. Kim, and W. Deppert, "Redox factor 1 (ref-1) enhances specific dna binding of p53 by promoting p53 tetramerization," *Oncogene*, vol. 24, no. 9, pp. 1641–7, 2005.

[65] D. P. Teufel, S. M. Freund, M. Bycroft, and A. R. Fersht, "Four domains of p300 each bind tightly to a sequence spanning both transactivation subdomains of p53," *Proc Natl Acad Sci U S A*, vol. 104, no. 17, pp. 7009–14, 2007.

[66] J. van Dieck, M. R. Fernandez-Fernandez, D. B. Veprintsev, and A. R. Fersht, "Modulation of the oligomerization state of p53 by differential binding of proteins of the s100 family to p53 monomers and tetramers," *J Biol Chem*, vol. 284, no. 20, pp. 13 804–11, 2009.

[67] R. S. Foo, Y. J. Nam, M. J. Ostreicher, M. D. Metzl, R. S. Whelan, C. F. Peng, A. W. Ashton, W. Fu, K. Mani, S. F. Chin, E. Provenzano, I. Ellis, N. Figg, S. Pinder, M. R. Bennett, C. Caldas, and R. N. Kitsis, "Regulation of p53 tetramerization and nuclear export by arc," *Proc Natl Acad Sci U S A*, vol. 104, no. 52, pp. 20 826–31, 2007.

[68] T. Kawaguchi, S. Kato, K. Otsuka, G. Watanabe, T. Kumabe, T. Tominaga, T. Yoshimoto, and C. Ishioka, "The relationship among p53 oligomer formation, structure and transcriptional activity using a comprehensive missense mutation library," *Oncogene*, vol. 24, no. 46, pp. 6976–81, 2005.

[69] F. P. Li, J. Fraumeni, J. F., J. J. Mulvihill, W. A. Blattner, M. G. Dreyfus, M. A. Tucker, and R. W. Miller, "A cancer family syndrome in twenty-four kindreds," *Cancer Res*, vol. 48, no. 18, pp. 5358–62, 1988.

[70] E. L. DiGiammarino, A. S. Lee, C. Cadwell, W. Zhang, B. Bothner, R. C. Ribeiro, G. Zambetti, and R. W. Kriwacki, "A novel mechanism of tumorigenesis involving ph-dependent destabilization of a mutant p53 tetramer," *Nat Struct Biol*, vol. 9, no. 1, pp. 12–6, 2002.

[71] A. Willis, E. J. Jung, T. Wakefield, and X. Chen, "Mutant p53 exerts a dominant negative effect by preventing wild-type p53 from binding to the promoter of its target genes," *Oncogene*, vol. 23, no. 13, pp. 2330–8, 2004.

[72] A. de Vries, E. R. Flores, B. Miranda, H. M. Hsieh, C. T. van Oostrom, J. Sage, and T. Jacks, "Targeted point mutations of p53 lead to dominant-negative inhibition of wild-type p53 function," *Proc Natl Acad Sci U S A*, vol. 99, no. 5, pp. 2948–53, 2002.

[73] J. L. Waterman, J. L. Shenk, and T. D. Halazonetis, "The dihedral symmetry of the p53 tetramerization domain mandates a conformational switch upon dna binding," *EMBO J*, vol. 14, no. 3, pp. 512–9, 1995.

[74] T. S. Davison, P. Yin, E. Nie, C. Kay, and C. H. Arrowsmith, "Characterization of the oligomerization defects of two p53 mutants found in families with li-fraumeni and li-fraumeni-like syndrome," *Oncogene*, vol. 17, no. 5, pp. 651–6, 1998.

[75] Y. Itahana, H. Ke, and Y. Zhang, "p53 oligomerization is essential for its c-terminal lysine acetylation," *J Biol Chem*, vol. 284, no. 8, pp. 5158–64, 2009.

[76] L. J. Warnock, A. Knox, T. R. Mee, S. A. Raines, and J. Milner, "Influence of tetramerisation on site-specific post-translational modifications of p53: comparison of human and murine p53 tumor suppressor protein," *Cancer Biol Ther*, vol. 7, no. 9, pp. 1481–9, 2008.

[77] J. M. Stommel, N. D. Marchenko, G. S. Jimenez, U. M. Moll, T. J. Hope, and G. M. Wahl, "A leucine-rich nuclear export signal in the p53 tetramerization domain: regulation of subcellular localization and p53 activity by nes masking," *EMBO J*, vol. 18, no. 6, pp. 1660–72, 1999.

[78] Y. Chen, J. D. Muller, P. T. So, and E. Gratton, "The photon counting histogram in fluorescence fluctuation spectroscopy," *Biophys J*, vol. 77, no. 1, pp. 553–67, 1999.

[79] Y. Chen, J. D. Muller, Q. Ruan, and E. Gratton, "Molecular brightness characterization of egfp in vivo by fluorescence fluctuation spectroscopy," *Biophys J*, vol. 82, no. 1 Pt 1, pp. 133–44, 2002.

[80] Y. Chen, L. N. Wei, and J. D. Muller, "Unraveling protein-protein interactions in living cells with fluorescence fluctuation brightness analysis," *Biophys J*, vol. 88, no. 6, pp. 4366–77, 2005.

[81] Y. Chen, J. D. Muller, K. M. Berland, and E. Gratton, "Fluorescence fluctuation spectroscopy," *Methods*, vol. 19, no. 2, pp. 234–52, 1999.

[82] M. Beam, M. C. Silva, and R. I. Morimoto, "Dynamic imaging by fluorescence correlation spectroscopy identifies diverse populations of polyglutamine oligomers formed in vivo," *J Biol Chem*, vol. 287, no. 31, pp. 26 136–45, 2012.

[83] Y. Chen, B. Wu, K. Musier-Forsyth, L. M. Mansky, and J. D. Mueller, "Fluorescence fluctuation spectroscopy on viral-like particles reveals variable gag stoichiometry," *Biophys J*, vol. 96, no. 5, pp. 1961–9, 2009.

[84] J. V. Fritz, P. Didier, J. P. Clamme, E. Schaub, D. Muriaux, C. Cabanne, N. Morellet, S. Bouaziz, J. L. Darlix, Y. Mely, and H. de Rocquigny, "Direct vpr-vpr interaction in cells monitored by two photon fluorescence correlation spectroscopy and fluorescence lifetime imaging," *Retrovirology*, vol. 5, p. 87, 2008.

[85] N. Kahya, D. Scherfeld, K. Bacia, B. Poolman, and P. Schwille, "Probing lipid mobility of raft-exhibiting model membranes by fluorescence correlation spectroscopy," *J Biol Chem*, vol. 278, no. 30, pp. 28 109–15, 2003.

[86] T. Weidemann, R. Worch, K. Kurgonaite, M. Hintersteiner, C. Bokel, and P. Schwille, "Single cell analysis of ligand binding and complex formation of interleukin-4 receptor subunits," *Biophys J*, vol. 101, no. 10, pp. 2360–9, 2011.

[87] Y. Chen, L. N. Wei, and J. D. Muller, "Probing protein oligomerization in living cells with fluorescence fluctuation spectroscopy," *Proc Natl Acad Sci U S A*, vol. 100, no. 26, pp. 15 492–7, 2003.

[88] K. Tarassov, V. Messier, C. R. Landry, S. Radinovic, M. M. Serna Molina, I. Shames, Y. Malitskaya, J. Vogel, H. Bussey, and S. W. Michnick, "An in vivo map of the yeast protein interactome," *Science*, vol. 320, no. 5882, pp. 1465–70, 2008.

[89] I. Remy, G. Ghaddar, and S. W. Michnick, "Using the beta-lactamase protein-fragment complementation assay to probe dynamic protein-protein interactions," *Nat Protoc*, vol. 2, no. 9, pp. 2302–6, 2007.

[90] C. D. Hu, Y. Chinenov, and T. K. Kerppola, "Visualization of interactions among bzip and rel family proteins in living cells using bimolecular fluorescence complementation," *Mol Cell*, vol. 9, no. 4, pp. 789–98, 2002.

[91] T. K. Kerppola, "Design and implementation of bimolecular fluorescence complementation (bifc) assays for the visualization of protein interactions in living cells," *Nat Protoc*, vol. 1, no. 3, pp. 1278–86, 2006.

[92] A. P. Funnell and M. Crossley, "Homo- and heterodimerization in transcriptional regulation," *Adv Exp Med Biol*, vol. 747, pp. 105–21, 2012.

[93] T. Imagawa, T. Terai, Y. Yamada, R. Kamada, and K. Sakaguchi, "Evaluation of transcriptional activity of p53 in individual living mammalian cells," *Anal Biochem*, vol. 387, no. 2, pp. 249–56, 2009.

[94] B. Schumacher, J. Mondry, P. Thiel, M. Weyand, and C. Ottmann, "Structure of the p53 c-terminus bound to 14-3-3: implications for stabilization of the p53 tetramer," *FEBS Lett*, vol. 584, no. 8, pp. 1443–8, 2010.

[95] T. Weidemann and P. Schwille, *Fluorescence Correlation Spectroscopy in Living Cells*. Dordrecht: Springer, 2009, ch. 8, pp. 217–241.

[96] P. Macdonald, J. Johnson, E. Smith, Y. Chen, and J. D. Mueller, "Brightness analysis," *Methods Enzymol*, vol. 518, pp. 71–98, 2013.

[97] T. R. Brummelkamp, R. Bernards, and R. Agami, "A system for stable expression of short interfering rnas in mammalian cells," *Science*, vol. 296, no. 5567, pp. 550–3, 2002.

[98] C. L. Brooks and W. Gu, "p53 regulation by ubiquitin," *FEBS Lett*, vol. 585, no. 18, pp. 2803–9, 2011.

[99] M. R. Fernandez-Fernandez, D. B. Veprintsev, and A. R. Fersht, "Proteins of the s100 family regulate the oligomerization of p53 tumor suppressor," *Proc Natl Acad Sci U S A*, vol. 102, no. 13, pp. 4735–40, 2005.

[100] T. E. Saunders, K. Z. Pan, A. Angel, Y. Guan, J. V. Shah, M. Howard, and F. Chang, "Noise reduction in the intracellular pom1p gradient by a dynamic clustering mechanism," *Dev Cell*, vol. 22, no. 3, pp. 558–72, 2012.

[101] G.-J. Kremers, J. Goedhart, E. B. van Munster, and T. W. J. Gadella, Jr, "Cyan and yellow super fluorescent proteins with improved brightness, protein folding, and fret förster radius," *Biochemistry*, vol. 45, no. 21, pp. 6570–80, May 2006.

[102] T. Nagai, K. Ibata, E. S. Park, M. Kubota, K. Mikoshiba, and A. Miyawaki, "A variant of yellow fluorescent protein with fast and efficient maturation for cell-biological applications," *Nat Biotechnol*, vol. 20, no. 1, pp. 87–90, Jan 2002.

[103] L. Cramer and T. J. Mitchison, "Moving and stationary actin filaments are involved in spreading of postmitotic ptk2 cells," *J Cell Biol*, vol. 122, no. 4, pp. 833–43, 1993.

[104] S. A. Kim, K. G. Heinze, and P. Schwille, "Fluorescence correlation spectroscopy in living cells," *Nat Methods*, vol. 4, no. 11, pp. 963–73, 2007.

[105] U. Alon, "Network motifs: theory and experimental approaches," *Nat Rev Genet*, vol. 8, no. 6, pp. 450–61, 2007.

[106] J. T. Mettetal, D. Muzzey, C. Gomez-Uribe, and A. van Oudenaarden, "The frequency dependence of osmo-adaptation in saccharomyces cerevisiae," *Science*, vol. 319, no. 5862, pp. 482–4, 2008.

[107] D. H. Kim, D. Grun, and A. van Oudenaarden, "Dampening of expression oscillations by synchronous regulation of a microrna and its target," *Nat Genet*, vol. 45, no. 11, pp. 1337–44, 2013.

[108] B. Vogelstein, D. Lane, and A. J. Levine, "Surfing the p53 network," *Nature*, vol. 408, no. 6810, pp. 307–10, 2000.

[109] L. Cai, C. K. Dalal, and M. B. Elowitz, "Frequency-modulated nuclear localization bursts coordinate gene regulation," *Nature*, vol. 455, no. 7212, pp. 485–90, Sep 2008.

[110] N. Hao and E. K. O'Shea, "Signal-dependent dynamics of transcription factor translocation controls gene expression," *Nat Struct Mol Biol*, vol. 19, no. 1, pp. 31–9, Jan 2012.

[111] J. E. Quintero, S. J. Kuhlman, and D. G. McMahon, "The biological clock nucleus: a multiphasic oscillator network regulated by light," *J Neurosci*, vol. 23, no. 22, pp. 8070–6, Sep 2003.

[112] G. M. Süel, J. Garcia-Ojalvo, L. M. Liberman, and M. B. Elowitz, "An excitable gene regulatory circuit induces transient cellular differentiation," *Nature*, vol. 440, no. 7083, pp. 545–50, Mar 2006.

[113] G. Gaglia, Y. Guan, J. V. Shah, and G. Lahav, "Activation and control of p53 tetramerization in individual living cells," *Proc Natl Acad Sci U S A*, vol. 110, no. 38, pp. 15 497–501, 2013.

[114] C. D. Hu, A. V. Grinberg, and T. K. Kerppola, "Visualization of protein interactions in living cells using bimolecular fluorescence complementation (bifc) analysis," *Curr Protoc Cell Biol*, vol. Chapter 21, p. Unit 21 3, 2006.

[115] C. Cohen-Saidon, A. A. Cohen, A. Sigal, Y. Liron, and U. Alon, "Dynamics and variability of erk2 response to egf in individual living cells," *Mol Cell*, vol. 36, no. 5, pp. 885–93, Dec 2009.

[116] G. H. Patterson, K. Hirschberg, R. S. Polishchuk, D. Gerlich, R. D. Phair, and J. Lippincott-Schwartz, "Transport through the golgi apparatus by rapid partitioning within a two-phase membrane system," *Cell*, vol. 133, no. 6, pp. 1055–67, Jun 2008.

[117] X. Chen, J. Chen, S. Gan, H. Guan, Y. Zhou, Q. Ouyang, and J. Shi, "Dna damage strength modulates a bimodal switch of p53 dynamics for cell-fate control," *BMC Biol*, vol. 11, p. 73, 2013.

[118] W. M. Chan, W. Y. Siu, A. Lau, and R. Y. C. Poon, "How many mutant p53 molecules are needed to inactivate a tetramer?" *Mol Cell Biol*, vol. 24, no. 8, pp. 3536–51, Apr 2004.

[119] P. Chene, "The role of tetramerization in p53 function," *Oncogene*, vol. 20, no. 21, pp. 2611–7, 2001.

[120] A. Lányi, D. Deb, R. C. Seymour, J. H. Ludes-Meyers, M. A. Subler, and S. Deb, "'gain of function' phenotype of tumor-derived mutant p53 requires the oligomerization/nonsequence-specific nucleic acid-binding domain," *Oncogene*, vol. 16, no. 24, pp. 3169–76, Jun 1998.

[121] P. Hainaut and J. Milner, "Interaction of heat-shock protein 70 with p53 translated in vitro: evidence for interaction with dimeric p53 and for a role in the regulation of p53 conformation," *EMBO J*, vol. 11, no. 10, pp. 3513–20, 1992.

[122] M. Wang, S. Qanungo, M. T. Crow, M. Watanabe, and A. L. Nieminen, "Apoptosis repressor with caspase recruitment domain (arc) is expressed in cancer cells and localizes to nuclei," *FEBS Lett*, vol. 579, no. 11, pp. 2411–5, 2005.

[123] L. T. Vassilev, B. T. Vu, B. Graves, D. Carvajal, F. Podlaski, Z. Filipovic, N. Kong, U. Kammlott, C. Lukacs, C. Klein, N. Fotouhi, and E. A. Liu, "In vivo activation of the p53 pathway by small-molecule antagonists of mdm2," *Science*, vol. 303, no. 5659, pp. 844–8, Feb 2004.

[124] N. Issaeva, P. Bozko, M. Enge, M. Protopopova, L. G. G. C. Verhoef, M. Masucci, A. Pramanik, and G. Selivanova, "Small molecule rita binds to p53, blocks p53-hdm-2 interaction and activates p53 function in tumors," *Nat Med*, vol. 10, no. 12, pp. 1321–8, Dec 2004.

[125] S. Lehmann, V. J. N. Bykov, D. Ali, O. Andrén, H. Cherif, U. Tidefelt, B. Uggla, J. Yachnin, G. Juliusson, A. Moshfegh, C. Paul, K. G. Wiman, and P.-O. Andersson, "Targeting p53 in vivo: a first-in-human study with p53-targeting compound apr-246 in refractory hematologic malignancies and prostate cancer," *J Clin Oncol*, vol. 30, no. 29, pp. 3633–9, Oct 2012.

[126] S. Y. Shieh, Y. Taya, and C. Prives, "Dna damage-inducible phosphorylation of p53 at n-terminal sites including a novel site, ser20, requires tetramerization," *EMBO J*, vol. 18, no. 7, pp. 1815–23, Apr 1999.

[127] T. R. Brummelkamp, S. M. B. Nijman, A. M. G. Dirac, and R. Bernards, "Loss of the cylindromatosis tumour suppressor inhibits apoptosis by activating nf-kappab," *Nature*, vol. 424, no. 6950, pp. 797–801, Aug 2003.

[128] Y. Sun, Z. Dong, T. Jin, K.-H. Ang, M. Huang, K. M. Haston, J. Peng, T. P. Zhong, S. Finkbeiner, W. A. Weiss, M. R. Arkin, L. Y. Jan, and S. Guo, "Imaging-based chemical screening reveals activity-dependent neural differentiation of pluripotent stem cells," *Elife*, vol. 2, p. e00508, 2013.